Stony Brook University

Microglia in the healthy and diseased central nervous system

A Dissertation Presented

by

Luisa Torres

to

The Graduate School

in Partial Fulfillment of the

Requirements

for the Degree of

Doctor of Philosophy

in

Molecular and Cellular Pharmacology

Stony Brook University

December 2014

Stony Brook University

The Graduate School

Luisa Torres

We, the dissertation committee for the above candidate for the

Doctor of Philosophy degree, hereby recommend

acceptance of this dissertation.

Stella Tsirka – Dissertation Advisor
Professor, Department of Pharmacological Sciences

Holly Colognato - Chairperson of Defense
Associate Professor, Department of Pharmacological Sciences

David Talmage- Committee Member
Professor, Department of Pharmacological Sciences

John K. Robinson- Outside Member
Professor, Department of Psychology

This dissertation is accepted by the Graduate School

Charles Taber
Dean of the Graduate School

Abstract of the Dissertation

The use of combinatory therapy for the treatment of spinal cord injury and the physiological role of microglia in the healthy central nervous system

by

Luisa Torres

Doctor of Philosophy

in

Molecular and Cellular Pharmacology

Stony Brook University

2014

Spinal cord injury (SCI) results in the death of neurons, disruption of neuronal connections, demyelination, and inflammation. There are three phases of SCI: Acute (from the time of impact to the first few days post-injury), secondary (hours to weeks), and chronic (months to years). Currently, little can be done to modify the acute phase. Efforts to intervene have focused on the subsequent phases to both promote healing and prevent further damage. In this study I show that the small molecule inhibitor Pifithrin-μ (PFT-μ) significantly reduced lesion volume and decreased the presence of inflammatory cells (microglia and macrophages) in the lesion site when applied during the acute phase of SCI. PFT-μ polarized microglia to the anti-inflammatory phenotype, and significantly improved motor coordination and posture in SCI animals when combined with the tripeptide microglia inhibitory factor (MIF/TKP), indicating that targeting both the acute and the secondary phase of SCI can facilitate repair and accelerate motor recovery.

In a parallel project I examined the behavioral outcomes resulting from elimination of microglia from the brain using a barrage of cognitive and social interaction tests. I show that microglia are dynamic regulators of such behaviors, a finding that confirms their modulatory role in the function of the Central Nervous System both in pathology and physiology.

Dedication Page

I dedicate this thesis to the loving memory of Dolly Duque and Roberto Duque, to my mother Gloria Duque, to my aunt Myriam Duque, and to my uncles Fernando Duque and Dario Duque.

Table of Contents

List of Figures and Tables

Preface

Microglia are the first line of defense against disease in the central nervous system (CNS). They originate from $CD45^{-}c\text{-}kit^{+}$ yolk-sac precursors that invade the brain using matrix metalloproteinases (MMPs), such as MMP-8 and MMP-9 [1]. These precursors eventually develop into $CD45^{+}c\text{-}kit^{-}CX3CR1^{+}$ microglia prior to the formation of the blood-brain barrier. During prenatal development microglia possess an ameboid shape and more closely resemble macrophages. Microglia then undergo proliferation and acquire ramified processes [2]. Once they fully colonize the brain parenchyma several factors including Colony Stimulating Factor -1 (Csf-1), Runx1, PU.1, Interferon Regulatory Factor 8 (IRF-8), and miR-124 contribute to their maintenance and self-renewal [2, 3].

Microglia play key roles in several neurological diseases and can quickly respond to infection or injury [4, 5]. Two-photon microscopy studies revealed that microglia use their processes to constantly survey the brain parenchyma ready to react to potential insults [6]. This perpetual surveying state allows microglia to serve important functions both under physiological and pathological conditions. In the healthy CNS, microglia phagocytose apoptotic cells, prune synapses, and support the formation of neural circuits [7, 8]. Under pathological conditions, microglia become activated and initiate an inflammatory response characterized by microglia proliferation, upregulation of a large number of microglial receptors, and cytokine production [4, 5, 9]. Besides their roles in mediating this inflammatory response, microglia also play an important supportive role in the CNS [2, 7, 10]. During early neurogenesis microglia phagocytose apoptotic cells and eliminate unwanted neuronal projections [7, 11]. They also control production of cortical neurons by regulating the proliferation and survival of neural

precursor cells [12-17]. Microglia provide trophic support for the formation of neuronal circuits and are indispensible for neuronal survival [8]. Microglia directly modulate synaptic activity by contacting synapses in a CR3/C3-dependent manner [7, 11, 18]. In co-cultures of neurons and microglia, microglia eliminate synapses via phagocytosis [11]. Neuronal stimulation results in extension of microglial processes towards highly active neurons, which in turn reduces neuronal activity [19].

Given the various supporting functions of microglia in the CNS, in this thesis I examine the role that microglia play in a pathological setting as well as under steady-state conditions. In chapter 3 I examine the microglia-driven inflammatory response in a mouse model of spinal cord injury and how this response can be modulated to improve anatomical and functional recovery. Finally, in chapter 4 I examine the behavior changes that occur upon elimination of microglia from the healthy brain using a variety of spatial and social memory tests. Microglia are shown to be dynamic players in both of these settings, a finding that confirms their modulatory role in the function of the CNS both in pathology and physiology.

Acknowledgments

I would like to thank my advisor, Dr. Stella Tsirka, for being my mentor and guide during these past five years. She became my graduate thesis advisor after I had to abruptly end my affiliation to a different lab. Stella was welcoming and supportive during that difficult time and helped me feel confident again about staying in the program. She made it easy for me to transition into her lab and has been a supportive mentor not only in my scientific training but also in regards to my personal life.

I thank my committee members Dr. Holly Colognato, Dr. David Talmage, and Dr. John Robinson for all their guidance and for the many meaningful discussions we have had. I thank them for helping me become a better scientist and for kindly guiding my work.

I thank the past and present members of the Tsirka lab, especially Dr. Noreen Bukhari and Dr, Jaime Emmetsberger for teaching me the contusion model of spinal cord injury, and Dr. Kyungmin Ji for being my go-to person, my mentor, and my friend. I thank my students Cyrus Rastegar, Nisha Rath, and Mike Caponegro for allowing me to mentor them and for helping me become a better teacher. I thank Cyrus and Nisha for their help quantifying the images for my spinal cord injury project. I thank Dr. Jillian Nissen for helping me adjust to the lab when I was first starting and for always being so kind when I ask for help. I thank Rob Bronstein for all his advice concerning several aspects of my research, and I thank Jeremy Miyauchi for his kind and happy spirit which has made my experience working in the lab a very memorable one.

I thank the Center for Inclusive education (Nina, Kathryne, and Toni) for all their help and support both during my time as a participant in their summer research program and during my

graduate school years. I thank the department staff, especially Odalis Hernandez for her friendship and help.

I thank my friend Maria Anderson for training me in all the behavior tests I performed for this dissertation work and Dr. Wahida Ali for being a great friend and wonderful mentor.

I thank all of my graduate and non-graduate student friends for always reminding me that there is life outside the lab. My last five years would not have been the same without their friendship and companionship. I also want to thank my flamenco instructor Juana Cala for being a wonderful teacher, and for helping me become a better dancer.

Lastly, I would like to thank my husband (Dr.) David for cheering me up when I felt down, for believing in me, and for supporting me in every way possible. I thank my mother Gloria for her unconditional love, for always making sure I stayed in school no matter the circumstances, and for teaching me the value of getting an education. I thank my step-dad Fernando for being a loving parent and for always offering me his support. I thank my uncle Fernando Duque for being present in all of my graduations, for helping my mom and I start a new life, and for helping me get through college with his generosity and kindness. I thank by grandfather Vicente Duque and my aunts Miriam Duque and Dolly Duque for their unconditional love and for making sure I grew up in a home surrounded by love and positivity. Finally, I thank my uncles Dario Duque and Roberto Duque, from whom I received such positive influence and who set a great example for me to follow.

Chapter 1: Introduction

Epidemiology of spinal cord injury

The National Spinal Cord Injury Database estimates that 12,000 cases of spinal cord injury (SCI) occur in the United States each year. This permanent debilitating condition results from a sudden impact that crushes the spinal tissue causing the instantaneous necrotic death of neurons and glia at the site of injury and disrupting the conduction of sensory and motor signals between the brain and the body [20]. SCI sufferers experience significant functional and sensory deficits including paralysis, bladder dysfunction, cardiovascular complications, deep vein thrombosis, osteoporosis, pressure ulcers, upper urinary tract damage, renal insufficiency, and neuropathic pain [21-26]. Worldwide, SCI affects 15 to 40 people per million annually [20, 21]. The location and severity of the impact determines the degree of loss of sensory, motor, and autonomic functions.

Pathophysiology

There are three phases of SCI: Acute (seconds to hours after the injury), secondary (hours to weeks after the injury), and chronic (months to years after the injury) (Table 1-I). During the primary injury, a hemorrhagic lesion slowly expands as a result of the coalition of petechial hemorrhages, resulting in the progressive damage of spinal cord tissues [27]. A marked release of the excitatory neurotransmitter glutamate occurs, which reaches toxic levels by 15 minutes following insult [28, 29]. The subsequent intracellular accumulation of calcium within 30 minutes post injury contributes to cell death. Activation of calcium-dependent phospholipases ultimately results in blood flow reduction and disruption of the blood-brain barrier [30]. Extracellular potassium levels are also acutely elevated leading to conduction block in the spinal

cord due to the partial depolarization of neuronal segments [30]. Decreased vasculature, which starts at 1 hour post injury and lasts for up to 14 days, contributes to cell death by reducing oxygen delivery to tissues [31]. Free radicals then form as a consequence of insufficient oxygenation, which exacerbates cell loss by damaging proteins and plasma membrane components[32]. Over time, cell death expands symmetrically both rostrally and caudally to the lesion site[33]. Opening of the blood-spinal cord barrier occurs as early as 1 hour after injury and is associated with edema formation and leakage of proteins and cytokines into the periphery [31, 32]. $CD45^+$, $Gr1^+$ neutrophils appear at the lesion site 12 hours post injury and return to normal levels between 24 and 48 hours[34] . This neutrophil infiltration coincides with the influx of $CD11b^+$, $F4/80^+$ inflammatory monocytes, which invade the lesion site 12 hours after injury and then again 4 days later, reaching peak numbers between two and three weeks [35, 36]. Expression of matrix metalloproteinase 9 (MMP-9) in neutrophils contributes to this vascular permeability [37]. Blood derived leukocytes also infiltrate the lesion site and reach peak numbers from 12-96 hours post injury [38]. Chronic waves of leukocyte infiltration continue to occur indefinitely, leading to fibrosis and impaired tissue healing [38]. T- and B-lymphocytes infiltrate the lesion site within the first week and continue to invade chronically [39]. Infiltration of inflammatory cells leads to the release of reactive oxygen species, bradykinins, histamines, and nitric oxide, which play a direct role in the activation of the post-traumatic inflammatory response[32].

The local inflammatory response

Microglia, the resident immune cells of the CNS, play a central role in the inflammatory response that follows SCI. Microglia respond to adenosine triphosphate (ATP) and other

extracellular ions within minutes after injury via P2 receptors [40, 41]. The subsequent gene induction causes microglia to quickly migrate to the site of damage to remove cell debris and release pro-inflammatory cytokines which recruit macrophages to the injury site [9]. In experimental SCI, the pro-inflammatory cytokines Tumor Necrosis Factor -α (TNF-α), Interleukin 1β (IL-1β), and IL-6 are upregulated within the first hour post-injury [42]. Similarly, microglia-produced chemokines, such as (C-C) motif ligand 2 (CCL2), CCL3, C-X-C motif ligand 2/3 (CXCL2/3) and CXCL10 [43] are upregulated soon after injury and help recruit and activate peripheral polymorphonuclear leukocytes and monocytes [44-47].

Microglia exist in a continuum between two extreme states: The M1 or pro-inflammatory state characterized by production of TNF-α, IL-1β, and IL-6 [48, 49] , and the anti-inflammatory M2 state characterized by production of IL-10, Transforming growth factor-β (TGF- β), IL-4, and IL-14. In several injury models, M2 microglia have been deemed beneficial for cell regeneration and the remyelination of damaged axons [50, 51], while M1 microglia favor continued inflammation and tissue injury. Although both M1 and M2 microglia are present at the injury site, M1 microglia predominate for at least the first 28 days post injury [50]. While expression of M2 markers, such as CD206 and arginase remains significantly increased up to day 14 post SCI, expression of M1 markers such as iNOS and CD16/CD32 remains significantly upregulated through day 28. Furthermore, when M2 polarized microglia are injected into the injured spinal cord the cells show reduced expression of M2 markers and increased expression of M1 proteins, indicating a predominance of M1 signals at the injury site [50]. Subpopulations of M1 and M2 microglia can switch their phenotypes back and forth in response to molecular cues [52], although debate still exists concerning whether microglia exist as distinct populations of

M1 and M2 cells, or whether the same cells can reverse their phenotype depending on the signals they receive [50, 53].

Microglia remain at the spinal cord for months following injury and continue to release cytokines, chemokines, and growth factors [32, 54-56]. Although microglial activation results in the release of cytokines that can be harmful to other cells [57-59], microglia can also release anti-inflammatory mediators that may offset the harmful impact of pro-inflammatory cytokines. For example, microglia-produced Insulin Growth Factor -1 (IGF-1) reduces cell death caused by high levels of TNF-α [60]. Similarly, IL-4 induces expression of IGF-1 and reverses the inhibitory effects of Interferon- γ (IFN-γ) [61]. Whether inflammation is beneficial or harmful depends on the extracellular environment as well as on the timing at which inflammation occurs. Pro-inflammatory cytokines produced acutely after spinal cord injury result in secondary cell death [62, 63]. Suppressing the inflammatory response following SCI has been shown to reduce secondary injury and improve functional outcome [64, 65]. Early inhibition of microglia activation using minocycline attenuates chronic pain following SCI [66]. Similarly, inhibition of the pro-inflammatory cytokine, IL-1β or TNF-α during the first 72 hours post injury significantly reduces apoptosis [67, 68]. However, in the chronic phase of SCI microglia have regenerative effects, as grafting cultured microglia into the injured spinal cord promotes axonal re-growth into the lesioned area [69]. These effects may be due to the release of trophic factors such as nerve growth factor (NGF), neurotrophin-3 (NT-3), IL-1a, IL-10, brain derived neurotrophic factor (BDNF), and IGF-1. Reactive microglia are also active phagocytes that participate in the removal of degenerating axons and inhibitory myelin debris after SCI, thereby enhancing the regeneration of axons.

Cell death after SCI

Uncontrolled microglial activation damages neurons and oligodendrocytes, the latter being responsible for producing myelin, the protective coat that insulates and protects axons. Oligodendrocytes express both AMPA and NMDA receptors which makes them vulnerable to apoptosis induced by glutamate, of which microglia is a major source [70-73]. Under normal conditions, excess glutamate is cleared by glutamate transporters expressed mainly by astrocytes[32]. However, SCI elevates glutamate to cytotoxic levels [74]. The resulting influx of calcium ions into neurons and oligodendrocytes leads to activation of apoptotic pathways. Calcium overload is also responsible for formation of free radicals, nitric oxide, activation of proteases, and mitochondrial damage[32]. Microglia-derived TNF-α may exacerbate glutamate-mediated cell death through activation of NF-κB [32]. Oligodendrocyte loss causes axon demyelination, eventually affecting the axon's ability to effectively send electrical impulses and causing sensory and cognitive deficits [70]. Following SCI, approximately half of the oligodendrocyte population near the lesion is lost within the first 2 days [33, 75], while oligodendrocyte death continues to occur for at least 3 weeks after injury. Apoptotic cells are mostly concentrated at or near the lesion epicenter and have been found in close contact with both degenerating axons and microglia/macrophages [76]. Oligodendrocyte apoptosis leads to chronic demyelination and axon degeneration. The subsequent fiber and myelin sheath disruption is known as Wallerian degeneration, which is responsible for the motor and sensory deficits that accompany SCI [77]. Microglia accumulate in great numbers around demyelinated areas [78, 79] and are found in close contact with dying oligodendrocytes [80]. Major myelin proteins, such as Proteolipid Protein (PLP), can be detected within Iba-1^{+} microglia/macrophages. Some studies have shown a direct effect of microglia on oligodendrocyte apoptosis through the release of

reactive oxygen and reactive nitrogen species [81-83]. However, in vivo models of demyelination have shown that anti-inflammatory cytokines favor oligodendrocyte formation. In vivo depletion of M2 microglia reduced expression of Myelin Basic Protein (MBP) and Myelin Oligodendrocyte Glycoprotein (MOG) and reduced the number of nodes of Ranvier ten days after Lysolecithin injection [51]. Similarly, in vitro experiments using oligodendrocytes treated with conditioned media derived from M1 or M2 polarized microglia showed that only the conditioned media from M2 microglia induced oligodendrocyte differentiation [51, 84].

As part of the endogenous reparative response, oligodendrocyte loss is compensated by oligodendrocyte progenitor cells (OPCs) that migrate to the injury site to proliferate and differentiate into mature oligodendrocytes [85-87]. Formation of new oligodendrocytes has been observed starting at day seven post injury [75]. However, remyelination especially at chronic time points post injury is incomplete and inefficient as unmyelinated axons are observed for up to 450 days post SCI [88]. Parallel to remyelination of damaged axons, new blood vessels are formed which favors axonal sprouting around the lesion area. For instance, new blood vessels can secrete prostacyclin which can then bind to damaged neurons and increase axonal regeneration and functional repair after SCI [89].

Besides oligodendrocytes, motor neurons also undergo apoptosis, with motor neuron loss occurring at greater distances from the injury site compared to oligodendrocytes [33]. Both oligodendrocytes and motor neurons display a similar cell death pattern over time after SCI, indicating that both may have a common factor that makes them vulnerable to cell death, such as microglia-derived glutamate and oxidative stress [33].

Formation of the glial scar

The initial injury triggers a series of biochemical and cellular events that mediate secondary apoptotic cell death, cause demyelination, and trigger an inflammatory immune response [90, 91]. A contributing factor to secondary injury is reactive gliosis, defined as the accumulation of myelin debris and remnants of damaged axons that attract various types of glial cells to the site of injury. Immediately after SCI, the expression of TNF-α, IL-1β, Leukemia Inhibitory Factor (LIF), and Cilliary Neurotrophic Factor (CNTF) is increased, which in turn increases proliferation of astrocytes as well as expression of the astrocytic marker Glial fibrillary acid protein (GFAP). Other cytokines known to increase astrocyte proliferation include TGF-β[92], INF-γ [93], IL-1[94], and IL-6[95]. Astrocytes undergo hypertrophy during the first few days post SCI and migrate towards the site of the lesion forming a dense cellular network known as the glial scar, which consists predominantly of reactive astrocytes, microglia/macrophages, OPCs, and extracellular matrix molecules such as laminin, fibronectin, and collagen [96]. The scar formation process seems to be dependent on Signal Transducer and Activator of Transcription 3 (STAT3) signaling as specific deletion of STAT3 in astrocytes leads to reduced astrocyte hypertrophy and abnormal scar formation[97]. β-catenin signaling also contributes to scarring as reducing OPC proliferation after spinal cord injury through deletion of β-catenin specifically in OPCs leads to reduced astrocyte hypertrophy [98].

The scar components seal the lesion and separate the injured areas from the spared tissue, thus preventing the spread of damage to distant sites. Reducing the migratory capacity of astrocytes results in increased infiltration of inflammatory cells, neuronal death, and motor deficits [97, 99]. Ablation of astrocytes reduces the expression of glutamate transporters and increases neuronal

loss, indicating a role for astrocytes in functional and anatomical repair after SCI [100]. In addition, astrocytes can secrete neurotrophic factors such as neurotrophin, CNTF [101], and IGF-1, the latter being crucial for successful remyelination and oligodendrocyte survival [102, 103]. Astrocytes can also secrete molecules that favor axon growth such as laminin and fibronectin [104] and can attract microglia/and macrophages to demyelinating lesions through release of the chemokine CCL1 [105]. Crosstalk between microglia and astrocytes is required for the neuroprotective functions of astrocytes [106]. In vitro experiments show that astrocytes are unable to respond to Lipopolysaccharide (LPS) stimulation in the absence of microglia and that microglia-derived TNF-α is required to induce production of neurotrophic factors in astrocytes [106].

In spite of the beneficial effects, the glial scar is rich in molecules that are inhibitory for repair [107, 108]. Examples of such molecules include Chondroitin Sulfate Proteoglycans (CSPGs) whose deposition occurs within 24 hours post SCI and is associated with reduced axonal re-growth [109-112] . In culture, CSPGs interfere with the adhesion, differentiation, and myelin protein production in human and mouse OPCs [107]. Enzymatic degradation of CSPGs using Chondroitinase reverses these effects and increases OPC migration, axonal sprouting, and remyelination in a model of spinal cord injury and in mice demyelinated with Lysolecithin [107, 113, 114]. These effects are accompanied by functional improvements [115, 116]. Chondroitinase can also induce an anti-inflammatory, phagocytic phenotype in microglia [117-119]. Other inhibitory molecules include Semaphorins, Slit proteins, and myelin proteins such as Myelin Associated Glycoprotein (MAG) and Oligodendrocyte Myelin Glycoprotein (OMG), all of which prevent the penetration of growing neurites into the lesion core [96, 120].

Therapeutic approaches

Repair from spinal cord injury (SCI) requires the coordinated action of different cells in the injured tissue: Microglia/macrophages must clear debris at the SCI site and promote an anti-inflammatory environment, oligodendrocyte precursors must differentiate to replace lost oligodendrocytes, and damaged axons must be repaired to re-establish spinal cord function. A number of anti-inflammatory drugs have been used in animal studies to reduce microglial activation and improve disease outcome. Our lab has shown that targeting microglial function during the secondary phase of spinal cord injury improves the injury outcome by enhancing oligodendrocyte differentiation and remyelination [65, 121]. The tripeptide MIF/TKP (tuftsin fragment 1-3, Thr-Lys-Pro) is a degradation product of the second constant domain of immunoglobulin G (IgG) that decreases phagocytosis and superoxide anion generation in peripheral macrophages and microglia (Figure 1-I, A) [122]. Treatment with MIF/TKP inhibits microglial activation, reduces axonal degeneration and lesion size, increases neurite outgrowth, enhances the proliferation of purified $NG2^+$ OPCs and their differentiation into mature cells, and reduces oligodendrocyte apoptosis in the hemisection model of SCI [65]

In this work, I use MIF/TKP in combination with 2-phenylethynesulfonamide (Figure 1-I, B), a small molecule inhibitor also known as Pifithrin- μ (PFT-μ), to assess the effects of combination treatment on lesion volume, microglial activation, and functional recovery in the contusion model of SCI. PFT-μ was isolated from a library of compounds known to modulate apoptosis [123] and was shown to inhibit the association of p53 with mitochondria by reducing its affinity for apoptotic proteins BcL-xL and Bcl-2 without affecting the transcriptional activity of p53 [123]. Inhibiting the association of p53 with mitochondria using PFT-μ results in reduced

mitochondrial release of cytochrome c and caspase-3 activation, reduced lesions, reduced neuronal damage, and improved motor and congnitive function in a model of perinatal hypoxic-ischemic brain damage [124]. In this model PFT-μ had a therapeutic window of six hours, indicating that PFT-μ acts acutely in this model to produce these beneficial effects. There is currently no effective treatment to target the acute phase of SCI. In this chapter I show that PFT-μ treatment significantly reduces lesion size and reduces the presence of microglia in the injury site. Combination of PFT-μ with MIF/TKP polarizes microglia to the M2 phenotype in vitro, reduces lesion volume, and significantly improves functional recovery, indicating that targeting both the acute and the secondary phases of injury results in improved histopathological and behavioral outcomes.[6]

Table 1-I: Stages of SCI

Acute Stage (1-2 days)	Secondary Stage (3-14days)	Chronic Stage (days-months)
Hypoxia and free radical formation	Macrophage infiltration	Continued demyelination and Wallerian degeneration
Intracellular calcium overload and cell death	Formation of astrogliotic scar	Continued apoptosis
Neutrophil invasion	Lesion stabilization	Regenerative processes
Hemorrhage and edema	Demyelination	
Opening of the BSB	Secondary cell death	
Release of cytokines and chemokines		

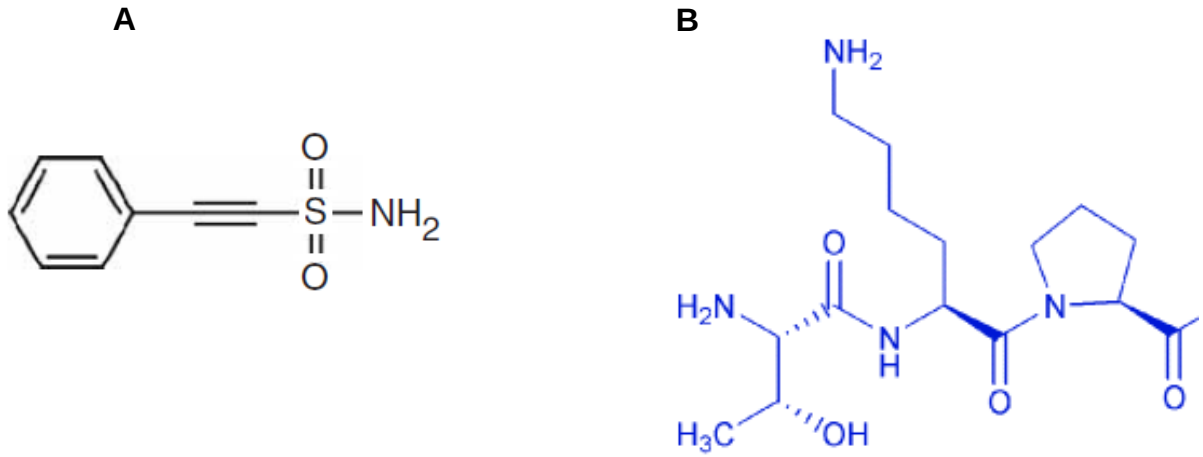

Figure 1-I: Chemical structures of (A) PFT-μ and (B) MIF/TKP

Chapter 2: Materials and Methods

Chapter 3

Contusion model of spinal cord injury: All experiments have been approved by the Institutional Animal Care and Use Committee (IACUC) and the Department of Laboratory Animal Research. Adult, age- matched C57BL/6 (wild-type) mice weighing 20-30g were anesthetized with Isoflurane. A dorsal laminectomy was performed between thoracic levels 8-10. The muscle and bone surrounding the spinal column were cut. A drill was used to decrease the thickness of the vertebrae and the remaining bone was removed with forceps and a micro-scissor. An impactor tip with 1.25mm in diameter was applied from a height of 2.5cm and a force of 50 kdynes using an Infinite Horizon Impactor (Precision Systems and Instrumentation). The overlying muscle and skin were sutured. Sham-operated groups underwent laminectomy without contusion. Postoperatively, mice were injected with buprenorphine (0.03 mg/kg) to reduce pain and placed on a heating pad overnight. Bladder expression was performed twice daily or until the mice regained bladder control. Mice were injected with a 5% dextrose/saline solution to prevent extreme weight loss. Animals that dropped more than 10% of their body weight, or that showed signs of limb or tail autophagy, were removed from the analysis.

Drug administration: Pifithrin-μ (PFT-μ, Sigma) was administered intraperitoneally at a dose of 8mg/kg body weight immediately after SCI [124]. 4% DMSO in PBS was used as vehicle. 100 μg/ml of MIF/TKP was administered via a 14-day micro-osmotic pump (Alzet. rate of infusion: 0.25 μl/h, 100 μl total volume). For experiments in which the effect of both drugs was tested on SCI outcome, PFT-μ was administered intraperitoneally

immediately after SCI followed by implantation of the osmotic pump containing 100 μg/ml MIF/TKP.

Pump preparation and implantation: 14-day osmotic pumps (Alzet) were filled with 100 μg/ml MIF/TKP prepared in sterile PBS and placed in 15 ml conical tubes containing sterile PBS. The pumps were placed at 37 ° C overnight to ensure that the pumping rate reached a steady state prior to use. Immediately after contusion injury the pumps were placed under the skin and the catheter tubing was sutured under the muscle so that the contents were delivered directly to the lesion site. The skin was sutured and mice were given buprenorphine and placed on a heating pad overnight. The pumps were removed 14 days after.

Perfusion and tissue collection: Mice were deeply anesthetized with 2.5% avertin and transcardially perfused with PBS followed by 4% PFA. The brain from microglia-depleted animals or the spinal cord from injured animals was collected, postfixed, and transferred to a 30% sucrose solution for cryoprotection. The brains were then frozen in OCT and sectioned into slices 40μm thick. The spinal cords were also frozen in OCT and cut into 20μm-thick slices.

Immunofluorescence: Immunofluorescence was performed on spinal cord as well as brain tissue. Sections were blocked for one hour with blocking solution (3% BSA and 0.02% triton-X100 in PBS) and then incubated with primary antibodies overnight at 4^{o}C The primary antibodies used were: Iba-1 (Wako, 1:500), GFAP (Cell Signaling,1:1000), NeuN (Millipore,1:100), and Collagen IV (Abcam, 1:500) . Sections were washed and

incubated with the appropriate secondary antibodies for one hour. Slides were washed and mounted with Dapi fluoromount.

Quantification of lesion volume and E-GFP intensity: To analyze lesion volume alternating sagittal spinal cord sections were stained with the astrocytic marker GFAP or collagen IV. Lesion size was analyzed from digital images of five alternate sections that had been immunofluorescently stained as described above. An observer blind to the treatment group used ImageJ software to calculate the area occupied by the lesion. The lesion was defined as the area bordered by $GFAP^+$ signal. In the case of collagen staining, the lesion site was defined as the area occupied by positive staining.

To quantify microglial infiltration into the lesion site, tissue sections from injured MacGreen mice were stained for Collagen IV to identify the injury epicenter. The area occupied by GFP^+ signal contained in the lesion site was selected and fluorescence intensity was measured by an observer blind to the treatment group using ImageJ. Data from each time point and treatment group were compared using the two-way ANOVA statistical method.

Primary neonatal microglial cell cultures: Cerebral cortices from postnatal day 1 C57BL/6J mice were dissected, digested with trypsin (0.25% in HBSS) for 15 mins at 37^oC, and mechanically dissociated by trituration as described in [125]. Mixed cortical cells were plated on poly-D-lysine coated tissue culture plates containing DMEM medium, 10% FBS, 1% sodium pyruvate, and gentamycin. After 10 days microglial cells were separated from the astrocytic monolayer by the addition of 12mM lidocaine, and the isolated microglia were seeded on 24 well plates at a density of 15,000 cells/ml

Enzyme Linked Immuno-Absorbent Assay (ELISA): Conditioned media from primary cell cultures was used for ELISA analysis. Cells were lysed to determine total protein concentrations and used for normalization of the data. Levels of TNF-α, IL-10, and TGF-β were determined using the eBiosciences quantitative sandwich enzyme immunoassay following the manufacturer's protocol. Briefly, 96 well plates were coated with diluted Capture antibody and incubated overnight at 4°C. The plates were blocked for one hour at room temperature followed by a two-hour incubation with standard or sample. The wells were then incubated for 1 hr with working detector solution followed by incubation with substrate solution for 30 min. The reaction was stopped with 50 µl of 1N H2SO4. The absorbance of each well was read at a 450 nm light wavelength. Data were normalized to total protein concentration.

Animal behavior

Rotarod test Motor performance was assessed in intact and injured mice using a Rotarod (Med Associates, Inc.) as described in [121] .Briefly, mice were placed on a moving rod that accelerated from 4 to 40 RPM over the course of five minutes. Once the mouse fell off, both the speed of the rod and the latency to fall were automatically recorded by the apparatus. Mice were subjected to three consecutive trials and the average of the trials was used for subsequent analysis. Rotarod performance was recorded at days 7, 14, 21 and 30 after contusion injury.

Footprint analysis The footprint test was used to assess gait and posture in spinal cord injured animals. To obtain footprints, both the forelimbs and hindlimbs of the mice were coated with black non-toxic ink. The animals were allowed to walk along a 50-cm-long, 10-cm-wide strip of filter paper (with 10-cm-high walls) as described in [126, 127]. Footprints were collected on days 7 and 30 post spinal cord injury. Three parameters were analyzed (all measured in

centimeters): (1) Stride length was measured as the perpendicular distance between each left or right forelimb stride. (2) front-base width was measured as the distance between front footprints. (3) hind paw base was measured as the distance between back footprints. For each parameter, five sets of footprints were measured from each mouse. The first and last set of footprints were excluded because they corresponded to footprints made when the animal was initiating and terminating movement, respectively. The mean value of each set of three values was used in subsequent analysis.

Chapter 6

Intrahippocampal clodronate injection: Injections were performed bilaterally in the hippocampus. Mice were deeply anesthetized with 1.25% Avertin. A small burr hole was made at stereotaxic coordinates (Stoelting, Wood Dale, IL) -2.5 mm from bregma and -1.7 mm lateral. 2 µl of phosphate buffered saline (PBS) or 2 µl of 10 mg/ml clodronate disodium salt (Calbiochem) in PBS were injected using a Hamilton syringe (0.485 mm I.D., Hamilton, Reno, NV) at a depth of 1.6 mm over 10 minutes with a motorized stereotaxic injector (Stoelting, Wood Dale, IL). To prevent reflux the needle remained in place for an extra five minutes. Following surgery, animals were injected intraperitoneally with 0.03 mg/kg of buprenorphine (Bedford labs) and left on a heating pad until they fully recovered from anesthesia.

Administration of the CSF-1R inhibitor (PLX3397): PLX3397 was obtained from Plexxikon Inc. and mixed into AIN-76A standard chow by Research Diets Inc. at the dose of 290 mg of drug per kg of chow [128]. Mice were fed with chow containing either vehicle (AIN-76A) or PLX3397 to deplete microglia.

Diaminobenzidine (DAB) staining of brain sections: DAB staining was performed on floating coronal sections using a modified protocol from previously established methods. Brain sections were washed with PBS and treated with 3% H_2O_2 for five minutes. Three- ten minute washes were performed with 1x PBS-T, followed by blocking with 1% BSA and incubation with the primary antibody (Iba-1, Wako: 1:500; GFAP, Abcam: 1:100) overnight. The sections were then washed and incubated with the appropriate secondary antibodies (biotinylated anti-rabbit IgG, Vector Laboratories). The ABC reagent was added (Vector Laboratories) for one hour. The sections were washed 3 times for 10 minutes with PBS-T. The signal was visualized using 3,3'-Diaminobenzidine (DAB) (Sigma Chemical Co) solution (DAB/0.1M PB/H2O2) until the desired strength was reached. The slices were removed from the wells, painted on slides and left to dry overnight. The sections were dehydrated in graded ethanol (50%, 70%, 90%, 100%, 100%), defatted in xylenes, and washed three times with 0.1M PB before mounting.

Cresyl violet staining: Fresh-frozen sections were dipped in 100% ethanol and washed in xylenes for two minutes. Serial hydration was performed in ethanol solutions ranging from 100% to 20%. The sections were then dipped in cresyl violet dye for 5 minutes, dipped twice in distilled water, and washed in 270 ml of 70% ethanol and 30 ml of 10% acetic acid. The sections were then dipped in 270 ml of 100% ethanol and 30 ml of 10% acetic acid, dehydrated with 100% ethanol, defatted in xylenes, and mounted.

Imaging: The DAB and cresyl violet stained sections were photographed under bright-field optics using a digital camera (Nikon CoolPix 990; Nikon, Tokyo, Japan) connected to a Nikon Eclipse E600 microscope. Immunofluorescently stained sections were photographed at a digital resolution of 1024 x 1024 with a Zeiss confocal microscope using LSM 510 Meta software

Animal behavior

Barnes maze: Barnes maze was performed to assess spatial memory after microglia depletion. Mice were placed on a circular maze containing eight equally spaced holes. An escape box was placed underneath a randomly selected hole. The amount of time taken by the mouse to find and enter the escape box (latency to find and latency to enter, respectively) and the total number of hole visits were recorded. The session ended when the mouse entered the escape box or after five minutes. Two trials were performed daily for five consecutive days. The test was conducted at the same time of the day throughout. Objects in the room were kept in the same position so that the mice could use them as spatial cues. The average latencies to find and enter the escape box were used for analysis.

Open field activity: Motor activity was measured using the Opto-Varimex-Minor animal activity meter (Columbus Instruments) as described in [121]. Mice were placed in an empty rat cage (44 cm x 21 cm) located inside the activity meter. Infrared beams (15 x 15) ran in the *x-y* coordinates. The total number of beams broken by the mouse as it moved around the cage as well as the animal's supported and unsupported motor movements (rearings) were recorded during the five- minute observation period.

Sociability and preference for social novelty: Sociability was measured in wild-type mice treated with clodronate or PLX3397 using the Crawley's sociability and preference for social novelty test described in [129]. A rectangular three-chamber box with an open middle section was used. Two identical wired cups were placed on each side of the chamber. The test was divided into two- ten minute sessions. In session 1, a mouse (stranger mouse1) was

placed under one of the wired cups, while the second wired cup located in the opposite chamber was left empty. The number of active contacts as well as the duration of the active contacts between the test mouse and both the empty cup and the cup containing stranger mouse 1 were recorded. An active contact was defined as any instance in which the mouse touched the wired cup with its snout or paws. In session 2, a second (novel) mouse was placed under the cup that had been empty during session 1. The number of active contacts as well as the duration of active contacts between the test mouse and both the familiar mouse and the novel mouse were recorded. Both Sessions were videotaped. The stranger mice and the subject mice were the same sex, weight, and age, but were not littermates of each other. This test was conducted every day for five days for the clodronate-treated animals and once on day 7 after administration of PLX3397.

Statistics: All statistics were performed using Statview (v4.0) or Graphpad Prism 6 for Windows, GraphPad Software (http://www.graphpad.com). Data are presented as mean ± SEM. Two-way ANOVA followed by Bonferroni's post hoc test was used to determine significance between experimental and control groups in the lesion volume analysis, E-GFP fluorescence intensity, and the motor behavior analysis. Pair-wise comparisons were made in the lesion volume analysis comparing the combination treatment to the vehicle treatment on day 30 post SCI. One-way ANOVA followed by Bonferroni's post-hoc test was used to analyze data from the ELISA assays. Mann-Whitney U test was used to determine significance between experimental and control groups in the Barnes maze test. Open field and social behavior were analyzed by Student's t-tests with Welch's correction for samples having possibly unequal variances. Data were considered statistically significant when $p < 0.05$

Chapter 3: The use of combinatory therapy for the treatment of SCI

Spinal cord injury (SCI) results in the death of neurons, disruption of neuronal connections, demyelination, and inflammation. There are three phases of SCI: Acute (from the time of impact to the first few days post-injury), secondary (hours to weeks), and chronic (months to years). Currently, little can be done to modify the acute phase. Efforts to intervene have focused on the subsequent phases to both promote healing and prevent further damage. In this chapter I show that the small molecule inhibitor Pifithrin-μ (PFT-μ) significantly reduced lesion volume and decreased the presence of inflammatory cells (microglia and macrophages) in the lesion site when applied during the acute phase of SCI. PFT-μ polarized microglia to the anti-inflammatory phenotype, and significantly improved motor coordination and posture in SCI animals when combined with MIF/TKP, indicating that targeting both the acute and secondary phase of SCI can facilitate repair and accelerate motor recovery.

MIF/TKP diffuses over the injury area

MIF/TKP effectively inhibited microglial activation both in vivo and in vitro in the hemisection model of SCI and remained stable at body temperature for up to 14 days [65]. To determine the location of MIF/TKP within the injured spinal cord, MIF/TKP was conjugated to a Rhodamine label and then administered *in vivo* via a 14-day micro-osmotic pump to injured MacGreen mice , which express E-GFP under the control of the microglia/macrophage promoter CSF-1R [130]. At 30 dpi mice were euthanized. Consistent with previous results, MIF/TKP is seen within the injury site closely associated with microglia/macrophages (Figure 3-I) [65]. Our lab had previously showed that MIF/TKP

diffused approximately 0.8 mm rostrally and 0.6 mm caudally to the lesion epicenter with the highest concentration of MIF present at the lesion core [65].

PFT-μ significantly reduces lesion volume 7 days post injury (dpi) both when applied alone and in combination with MIF/TKP

Environmental cues present at the SCI site induce astrocytes to undergo hypertrophy, proliferation, and migration, forming a dense cellular network that surrounds the epicenter of the lesion[104]. $GFAP^+$ astrocytes demarcate the lesion site and separate the injured tissue from spared areas. To determine the effect of PFT-μ on injury size, contused wild-type mice were given an i.p injection of 8mg/kg of PFT-μ and euthanized at day 7 or day 30 post SCI. This dose was chosen based on a previous report showing the protective effects of PFT-μ in a model of neonatal brain ischemia [124]. Spinal cord sections were immunofluorescently labeled with an anti-GFAP antibody and the area occupied by the lesion was quantified by an observer blind to the treatment group using ImageJ. The lesion site was defined as the area devoid of GFAP positive signal. Figure 3-II, A-B shows a significant reduction in lesion size with PFT-μ treatment compared to vehicle.

Collagen-producing fibroblasts also participate in the scar formation process by closely interacting with astrocytes [96]. $Collagen1\alpha^+$ fibroblasts begin accumulating on day 4 post SCI, become clearly visible by day 7, and persist up to day 56 post injury [131]. The same reduction in lesion volume is observed in tissue sections immunofluorescently labeled with an anti - Collagen IV antibody (Figure 3-III, A-B). In this case the injury site was defined as the area occupied by Collagen IV positive staining.

To test the effect of combining PFT-μ and MIF/TKP on lesion volume SCI mice received either an injection of 8mg/kg of PFT-μ, an osmotic pump containing 100 μg/mL of MIF/TKP, or both. Mice were euthanized at day 30 post injury, tissue sections were immunofluorescently labeled with an anti- Collagen IV antibody and lesion volume was analyzed as above. The combination treatment resulted in significantly smaller injuries compared to animals that received the control treatment (Figure 3-IV, A-B).

PFT-μ significantly reduces the presence of microglia in the lesion site at 30 dpi

Under steady state conditions, microglia use their processes to continuously scan the surrounding extracellular space and to communicate directly with glia, neurons, and blood vessels [6]. This surveying state allows them to respond quickly to damage or infection by transforming into an activated phenotype and turning on gene expression that ultimately leads to their proliferation and migration to the site of injury. To examine whether PFT-μ alters the presence of microglia at the lesion site, Macgreen mice underwent contusion SCI and received an i.p injection of 8mg/kg of PFT-μ. The animals were euthanized at day 7 and 30 post injury. Tissue sections were immunofluorescently labeled with an anti-Collagen IV antibody to delineate the lesion epicenter. An observer blind to the treatment group used ImageJ to quantify fluorescence intensity of the E-GFP signal contained within the lesion site. At day 7 post SCI, the intensity of E-GFP in the injury site was significantly stronger in both vehicle and PFT-μ-treated mice compared to that of sham controls (Figure 3-V, A-B). While the intensity of E-GFP signal after vehicle treatment remained significantly higher compared to control at day 30, the intensity of E-GFP in the injury site significantly decreased in PFT-μ-treated animals indicating a reduced microglia/macrophage presence with PFT-μ treatment (Figure 3-V, A-B). No significant difference was observed between mice that received MIF/TKP treatment alone and vehicle

treated animals or between mice that received a combination of PFT-μ and MIF/TKP and vehicle treated mice (Figure 3-VIII, A-B)

PFT-μ significantly reduces the expression of pro-inflammatory marker CD86

Microglia exist in a continuum between two extreme states: The M1 or pro-inflammatory state characterized by production of TNFα, IL-1β, and IL-6 [48, 49] , and the anti-inflammatory M2 state characterized by production of IL-10, TGF-β, IL-4, and IL-14. In several injury models, M2 microglia have been deemed beneficial for oligodendrocyte formation and the remyelination of damaged axons [50, 51], while M1 microglia favor continued inflammation and tissue injury. Although both M1 and M2 microglia are present at the injury site, several studies have reported that the presence of M2 microglia is only transient, while M1 microglia are predominant [50]. M1 microglia can be identified through a variety of markers including CD86, iNOS, CD16/CD32, while arginase-1, CD206, and Ym-1 can be used to indentify M2 cells [50]. To determine whether PFT-μ has an effect on microglial polarization tissue sections from vehicle treated and PFT-μ treated Macgreen mice from day 7 post injury were immunofluorescently labeled with either M1 marker CD86 or M2 marker CD206. Confocal images were taken from microglia located within the lesion site. Six images were taken per tissue section and five sections were imaged per biological replicate (Figure 3-VI). The percentage of microglia positive for either CD86 or CD206 was calculated over the total number of E-GFP$^+$ cells. Figure 3-VII (top) shows a significant decrease in the percentage of E-GFP$^+$ CD86$^+$ cells after PFT-μ treatment, while expression of CD206 remained unchanged. There was a decrease in the ratio of CD86$^+$ to CD206$^+$ cells and an increase in the ratio of CD206$^+$ to CD86$^+$ cells in the mice that received PFT-μ treatment compared to control, indicating a trend towards a phenotypic change from the M1 to the M2 state after PFT-μ treatment (Figure 3-VII, bottom).

PFT-μ polarizes cultured microglia to the anti-inflammatory M2 state

To characterize the effect of PFT-μ on the microglial production of pro-inflammatory and anti-inflammatory cytokines, microglia were cultured from the brain of neonatal wild-type mice according to the protocol described in [125]. Microglia were treated with PFT-μ at doses of 1, 3, and 5 μM. LPS was used as a positive control because it is a potent inducer of pro-inflammatory markers in microglia [132]. Six hours after treatment the media from the cells were collected, spun down, and used for ELISA. As expected, LPS significantly increased levels of TNF-α, whereas PFTμ did not affect TNF-α production at any of the doses examined (Figure 3-IX, A). Interestingly, PFT-μ was able to significantly decrease the LPS-induced TNF-α levels (Figure 3-IX, A). Combining PFT-μ and MIF/TKP produced the same effect. There was a dose-dependent increase in IL-10 levels with PFTμ which was significant over control treatment at the 5 μM dose (Figure 3-IX, B). Combining MIF/TKP with 1 μM PFT-μ resulted in significantly increased levels of IL-10 compared to control treatment (Figure 3-IX, B). I also found a dose-dependent decrease in the ratio of TNF-α to IL-10 (Figure 3-X, A) as well as a dose dependent increase in the ratio of IL-10 to TNF-α (Figure 3-X, B). There was a significant increase in the ratio of IL-10 to TNF-α between the 1 μM dose of PFT-μ and the 5 μM dose, and also between the 1 μM dose of PFT-μ and the combination of 1 μM PFT-μ and MIF/TKP (Figure 3-X,B). Together, this data indicate that PFTμ polarizes microglia to the M2 state under pro-inflammatory conditions.

PFTμ significantly improves motor coordination in SCI mice when applied in combination with MIF/TKP

Treatment with MIF/TKP results in reduced microglia activation, improved remyelination, reduced cell death, and increased axonal re-growth[65]. PFT-μ treatment reduces the presence of microglia into the lesion site, polarizes cultured microglia to the M2 phenotype, and reduces

lesion volume. To correlate these improved anatomical findings with improved behavioral outcomes, we used the Rotarod test and the footprint analysis to determine the effect of both drugs on functional recovery. The Rotarod test measures balance and motor coordination, while the footprint analysis measures posture and gait [133, 134]. To examine the effect of the combination treatment on functional recovery, wild-type mice underwent contusion injury and received either an injection of 8mg/kg of PFT-μ, an osmotic pump containing 100 μg/mL MIF/TKP, or both. To test the effect of treatment on motor coordination and balance, injured mice were tested on the Rotarod at days 7, 14, 21, and 30 post SCI as previously described [121]. At days 7 and 30 post injury, the combination treatment was significantly more effective at improving Rotarod performance compared to MIF/TKP treatment alone (Figure 3-XI). At days 14 and 21 post injury, injured mice that received the combination treatment showed a significant improvement in Rotarod performance compared to both PFT-μ and MIF/TKP, indicating that PFT-μ significantly improves motor coordination and balance when combined with MIF/TKP (Figure 3-XI).

To test the effect the combination treatment on posture and gait, injured mice were treated as above and subjected to footprint analysis. The forepaws and hindpaws of sham and injured mice were dipped in non-toxic ink and the mice were allowed to walk on a strip of filter paper as described in [126, 127]. Footprints were collected on days 7 and 30 post SCI. Figure 3-XII shows representative footprints from day 7 post injury. Three parameters were analyzed (all measured in centimeters): (1) Stride length was measured as the perpendicular distance between each left or right forelimb stride (Figure 3-XIII, A). (2) front-base width was measured as the distance between front footprints (Figure 3-XIII, B). (3) hind paw base was measured as the distance between back footprints (Figure 3-XIII, C). For each parameter, five sets of footprints

were measured from each mouse. The first and last set of footprints were excluded because they corresponded to the footprints made by the animal when it was initiating and terminating movement, respectively. Figure 3-XIII, A-B shows no significant difference in stride length or front-base width. However, there was a statistically significant difference in hind paw base between vehicle treated animals and mice treated with both PFT-μ and MIF/TKP at day 7 post injury (Figure 3-XIII, C). Together, these results indicate that the combination treatment significantly improves motor coordination and posture in SCI animals.

Discussion

Repair of the injured spinal cord remains challenging due to persistent inflammation, extensive cellular loss, inhibitory molecules present in the glial scar, and lack of factors that stimulate growth and repair. Accordingly, effective treatments should include combinatorial strategies to overcome the numerous limitations. There are several examples of effective drug combinations for the treatment of SCI in experimental models. For instance, Chondroitinase treatment together with rehabilitation training significantly improves motor function and increases axonal regeneration and synapse formation in SCI rats [115]. Chondroitinase treatment alone improves axonal sprouting but it is not enough to induce a significant improvement in motor function [121]. Similarly, rehabilitation training shows only modest improvements in functional recovery, indicating that the drug combination produces synergistic effects [115]. Treadmill training combined with implantation of neural stem cells into the injured area synergistically improves locomotor recovery in contused rats [135]. Engraftment of Schwann cells previously engineered to produce Neurotrophin and Chondroitinase significantly improves remyelination, axonal sprouting, and sensory and motor recovery [116].

In this work, I have used a combination of two drugs to test their effects on anatomical and functional repair after SCI. Previous work revealed that microglia inhibition using MIF/TKP results in improved axonal growth through the glial scar, smaller lesions, higher numbers of oligodendrocytes, and improved remyelination [65]. PFT-μ has been shown to have protective effects in two models of ischemic injury, but its effect in the context of spinal cord lesions has not been examined. Here I show that PFT-μ significantly reduces lesion size and downregulates the expression of pro-inflammatory markers including CD86 and TNF- α. In vitro stimulation of

microglia with PFT-μ did not elicit a strong inflammatory response in microglia as levels of TNF- α remained unchanged. However, PFT-μ significantly reduced LPS- induced TNF- α at all the doses examined. There was a dose-dependent increase in IL-10 levels with PFT-μ treatment as well as a dose-dependent increase in the ratio of IL-10 to TNF- α. A similar trend was observed in production of TGF-β although there were no significant differences (data not shown). The increase in IL-10 production could explain the observed reduction in lesion volume with PFT-μ treatment since this cytokine has been shown to attenuate astroglial reactivity [136]. IL-10 reduces secondary inflammation and pro-inflammatory cytokine production [137, 138], blocks the activation of NF-kB, and attenuates the synthesis of chemokines and matrix proteases, which might explain the reduced presence of microglia/macrophages in the injury site observed with PFT-μ treatment. The combination of PFT-μ and MIF/TKP resulted in smaller lesions, reduction of TNF-α after in vitro stimulation of microglia with LPS, increased IL-10 production, and a significant improvement in motor coordination and posture. This last finding was a synergistic effect as performance in the Rotarod and footprint analysis was significantly better in the injured mice that received the combination treatment compared to those that received either therapy alone.

PFT-μ has been shown to confer protective effects if applied within six hours of neonatal brain ischemia [124]. These protective effects were mediated by blocking the association of p53 with mitochondria and the subsequent cytochrome c release and activation of caspase 3. PFT-μ also reduced cell death, infarct size, and nuclear accumulation and activation of pro-apoptotic proteins PUMA and Noxa in a model of ischemic brain injury [139]. Here, we show that PFT-μ treatment immediately after injury results in significantly smaller injuries, reduced presence of microglia/macrophages in the injury site, and polarized microglia/macrophages to the anti-

inflammatory phenotype. p53 expression has been observed in neurons, microglia, oligodendrocytes, and astrocytes after SCI [140, 141]. p53 and Bax protein levels increase at 24 hours after SCI and remain upregulated for up to 21 days [140]. A second study reported expression of p53 within 30 minutes of SCI and up to 3 days post injury[141]. PFT-μ had protective effects when administered immediately after injury, while administration of the drug 24 hours after had no effect on lesion size or functional recovery (data not shown). Although the course of p53 expression was not examined in this work, given that it has been shown by others that p53 is upregulated at 24 hours after SCI it is unlikely that the protective effects of PFT-μ described here are due to the inhibition of the association between p53 and mitochondria. An alternative mechanism of action for PFT-μ is inhibition of heat shock protein 70 (hsp70) [142], a protein upregulated in cancer cells as a way to cope with nutrient shortage and accumulation of unfolded proteins [143]. Several studies have shown that PFT-μ can selectively kill cancer cells and enhance the effect of antitumor therapies [144-148]. Our findings that PFT-μ results in the polarization of microglia from an M1 to an M2 phenotype are consistent with a recent study that reports that PFT-μ reduces infiltration of inflammatory cells as well as expression of inflammatory markers such as TNF-α, IL-6, iNOS, and nitric oxide through inhibition of Hsp70 in a model of liver injury [149]. These results are also consistent with recent findings showing that PFT-μ reduces production of reactive oxygen species as well as cell death following excitotoxic challenge in the rat striatum [150]. However, in the context of SCI Hsp70 expression is beneficial as it protects glia and macrophages from the oxidative stress caused by the phagocytosis of cellular debris [151, 152]. Hsp70 expression has been reported in glia and macrophages reaching peak protein levels 24 hours after SCI [153]. Given that PFT-μ does not

seem to be effective if administered 24 hours after injury, it is also unlikely that PFT-μ is exerting its positive effects through inhibition of Hsp70.

Future directions

I have shown that combining PFT-μ and MIF/TKP to treat spinal cord injured mice results in smaller lesions, improved motor coordination and posture, reduced TNF-α release after in vitro stimulation of microglia with LPS, and increased IL-10 production by microglia. The in vivo beneficial effects of PFT-μ were observed when the drug was administered immediately after injury but not at 24 hours. For future experiments, it would be valuable to narrow down the therapeutic window of PFT-μ. In two models of brain ischemia PFT-μ had observable therapeutic effects if administered within 6 hours post injury [124, 139]. Since we observed beneficial effects of PFT-μ when given to SCI animals immediately after injury but not at 24 hours it is conceivable that PFT-μ will have a similar therapeutic window in our model of SCI. Whether the combination treatment produces the same effects when administered at different time points should also be determined. Studies suggest that inhibition of microglia early after injury is beneficial, while inhibition at later time points is detrimental. Microglia and macrophages persist for months in the injured spinal cord [32, 55] and continue to release cytokines, chemokines, and growth factors [56]. In the chronic phase of SCI microglia have regenerative effects, as grafting cultured microglia into injured spinal cord promotes axonal regrowth into the lesioned area [69]. These effects may be due to the release of trophic factors. Similarly, while inhibition of microglia using MIF/TKP early after injury results in reduced TNF-α release, enhanced IL-10 expression, and increased axonal growth through the glial scar, ablating microglia at later time points produces the opposite effect [65]. It should be studied whether administering MIF/TKP at later time points after injury is beneficial or detrimental for

functional recovery and whether combining it with PFT-μ furthers or reduces the beneficial effects.

The mechanism of action of PFT-μ should be determined. It is unlikely that PFT-μ is inhibiting the association of p53 to mitochondria or inhibiting the action of Hsp70 as described in other models given that the peak expression of p53 and Hsp70 does not coincide with the time window at which the beneficial effects of PFT-μ occur. Whether PFT-μ can bind to cell receptors that inhibit or activate signaling pathways or whether it can be internalized by cells and bind to intracellular proteins should be further investigated.

The signals that control microglia/macrophage polarization have not been identified. Two studies demonstrated that the extracellular environment after injury favors M1 activation [50, 53]. The development of the M2 phenotype depends upon the association of microglia/macrophages with inhibitory molecules such as extracellular matrix proteins and CSPGs [10]. Molecular switches that may control microglia/macrophage polarization include the Akt kinases, which have been shown to differentially regulate phenotypic changes in microglia [154]. Notch signaling has been shown to promote the M1 phenotype in macrophages through SOCS3 [155]. SOCS proteins negatively regulate JAK/STAT signaling, ultimately reducing inflammation [156]. SOCS1 can regulate the M1 phenotype by inhibiting the TLR/NF-κB signaling pathway. In contrast, expression of SOCS3 coincides with expression of pro-inflammatory markers such as iNOS [156]. LPS stimulation of microglia leads to activation of the PI3K/Akt pathway through Toll-like receptor-4 leading to activation of inflammatory pathways such as NF-κB [157]. In vitro experiments in which microglia previously exposed to PFT-μ are treated with inhibitors of these signaling cascades or with antibodies against specific

pathway components should be performed in order to dissect what pathways PFT-μ may be acting upon to downregulate M1 activation and promote the M2 phenotype.

Given that PFT-μ reduced the expression of pro-inflammatory markers such as TNF-α and CD 86 and increased expression of anti-inflammatory markers such as IL-10, it would be interesting to test the effect of PFT-μ on oligodendrocyte survival, OPC proliferation, and differentiation. Some studies have shown a direct effect of microglia on oligodendrocyte apoptosis through the release of reactive oxygen and reactive nitrogen species [81-83]. In microglia-oligodendrocyte co-cultures microglia can cause either survival or death of oligodendrocytes depending on the activation state of microglia as well as the differentiation state of the oligodendrocytes [158]. While inactive microglia protect OPCs [159], microglia and macrophages isolated from contused spinal cords inhibit OPC growth through the release of soluble factors [160]. Similarly, whereas cultured activated microglia reduce OPC survival, microglia seem to have a protective effect on mature oligodendrocytes regardless of their activation state [60, 161]. It was recently shown that $NG2^+$ OPCs take 48 hours to differentiate into $CC1^+$ oligodendrocytes during postnatal development, providing ample time for cues in the microenvironment to control oligodendrocyte differentiation [162]. Experiments with co-cultures of microglia and OPCs should be performed in order to determine the effect of PFT-μ and the subsequent IL-10 release by microglia on OPC survival, proliferation and differentiation into mature oligodendrocytes. OPC proliferation should be examined in vivo through immunofluorescent labeling of proliferating OPCs. Immunofluorescent labeling for apoptotic marker Caspase-3 and the oligodendrocyte marker CC1 should also be performed in order to assess the effect of PFT-μ on oligodendrocyte loss after SCI. Given that PFT-μ treatment has

reduced cell death in two models of brain ischemia, PFT-μ may lead to reduced oligodendrocyte loss after SCI.

Demyelinating lesions occur in the CNS as a result of oligodendrocyte death following CNS trauma. In response, OPCs proliferate and migrate towards the demyelinating region in an attempt to repair the damaged axons [85-87]. Whether PFT-μ promotes remyelination of damaged axons should be determined in future experiments using electron microscopy. Whether PFT-μ can increase axonal regeneration through the glial scar should be examined using axonal tracing techniques as well as in vitro neurite outgrowth assays. It should also be studied whether PFT-μ can reduce expression of inhibitory molecules present in the glial scar such as CSPGs, semaphorins, and Slit proteins.

Finally, PFT-μ significantly reduced lesion size as evidenced by smaller lesion areas bordered by GFAP-positive signal. More work should be conducted to determine the effect of PFT-μ on astrocyte proliferation, migration, and GFAP expression. In vitro experiments using isolated microglia showed a clear direct effect on microglia. Similar in vitro experiments should be conducted with astrocytes in culture to determine the effect of PFT-μ on astrocyte activity.

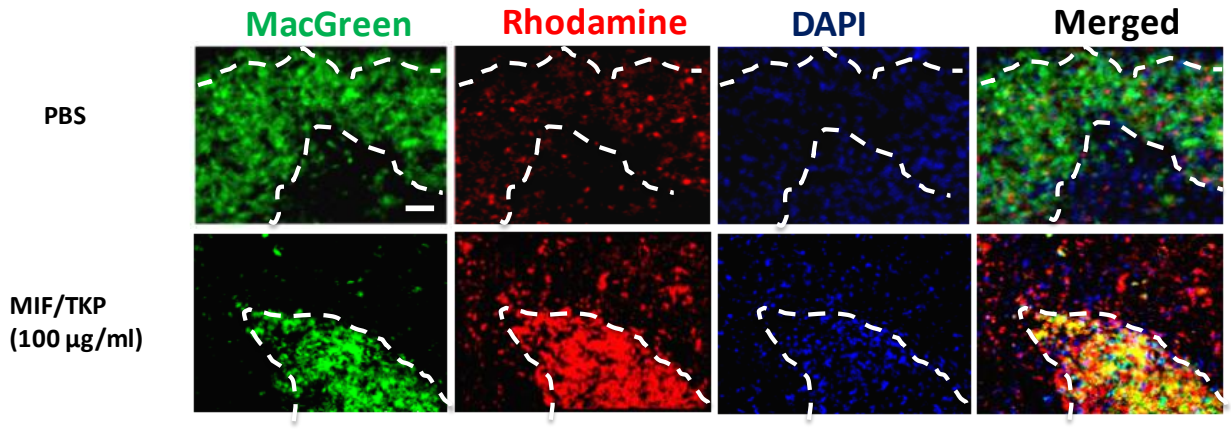

Figure 3-I: MIF/TKP diffuses over the injury area. Macgreen mice underwent contusion injury. An osmotic pump containing 100 µg/ml of Rhodamine-labeled MIF/TKP was sutured under the muscle on top of the injury site. Mice were euthanized at day 30 post injury. n=3 per group

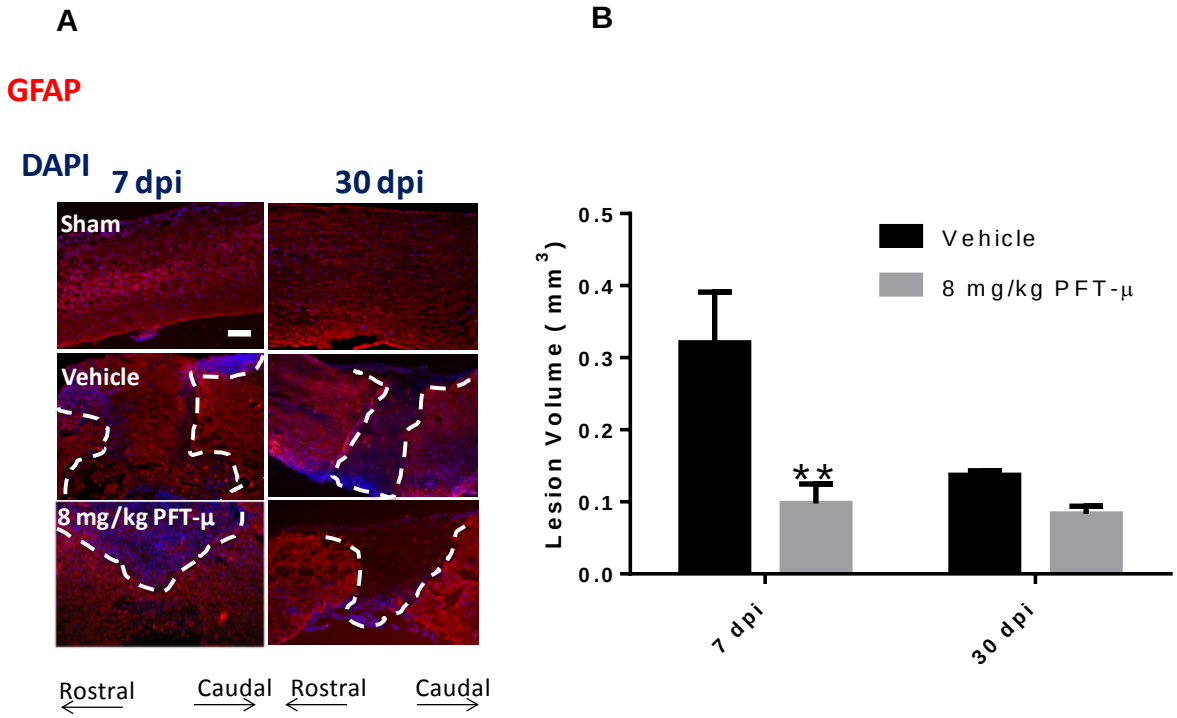

Figure 3-II: PFT-µ significantly reduces lesion volume. (A) Tissue sections from injured wild-type mice at day 7 and 30 post SCI were immunofluorescently labeled with the astrocytic marker GFAP. Dotted lines outline the lesion border. Scale bar = 200 µm. (**B)** Lesion volume was quantified by an observer blind to the treatment group using ImageJ. Sham controls underwent laminectomy without contusion. n= 3-7 per group. Data are shown as mean ± SEM. ** $p<0.01$.

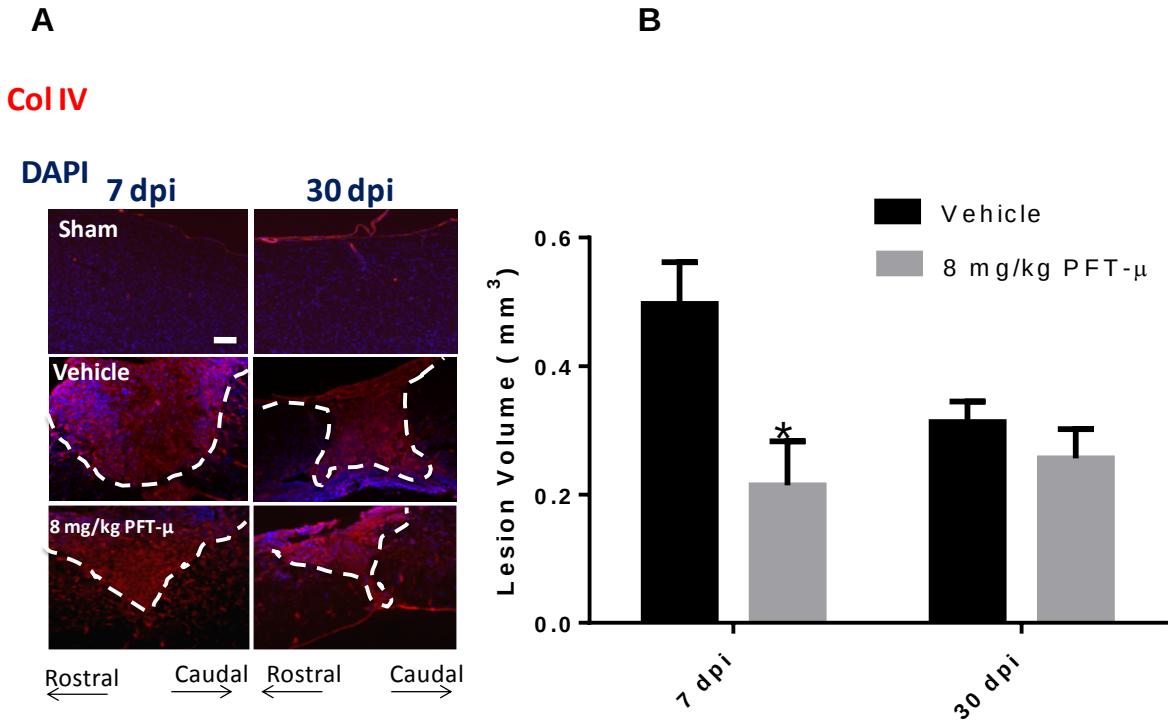

Figure 3-III: PFT-μ significantly reduces lesion volume. (A) Tissue sections from injured wild-type mice at day 7 and 30 post SCI were immunofluorescently labeled with an anti-Collagen IV antibody. Dotted lines outline the lesion border. Scale bar = 200 μm. **(B)** Lesion volume was quantified by an observer blind to the treatment group using ImageJ. Sham controls underwent laminectomy without contusion. n= 3-6 per group. Data are shown as mean ± SEM. *p<0.05

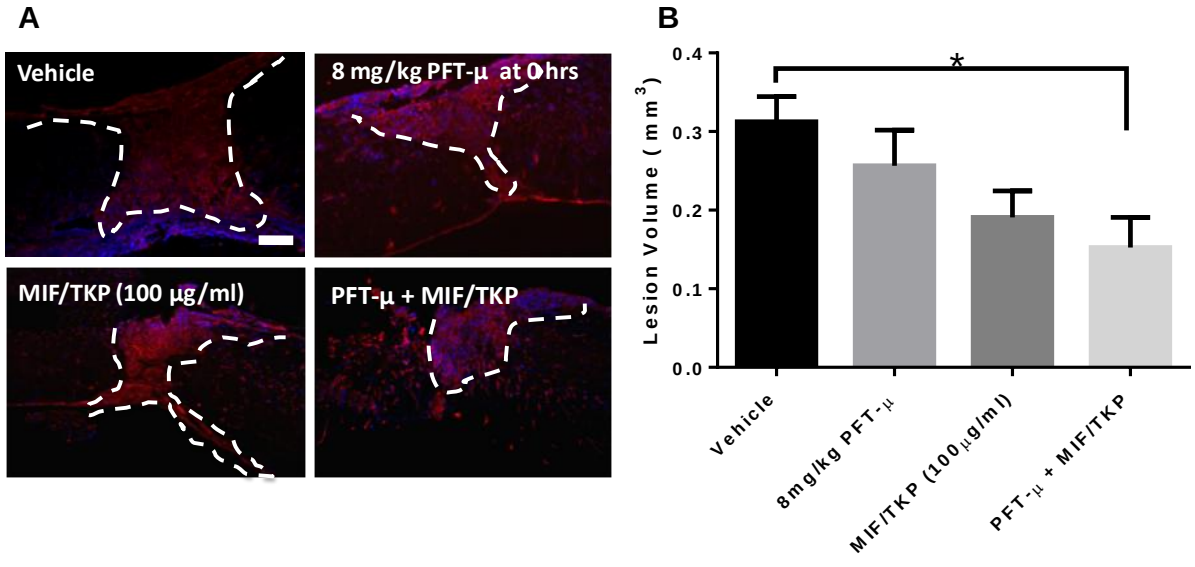

Figure 3-IV: PFT-μ significantly reduces lesion volume when combined with MIF/TKP. (A) Tissue sections from injured wild-type mice at day 30 post SCI were immunofluorescently labeled with an anti-Collagen IV antibody. Dotted lines outline the lesion border. Scale bar = 200 μm. (**B)** Lesion volume was quantified by an observer blind to the treatment group using ImageJ. n=3-6 per group. Data are shown as mean ± SEM. *p<0.05

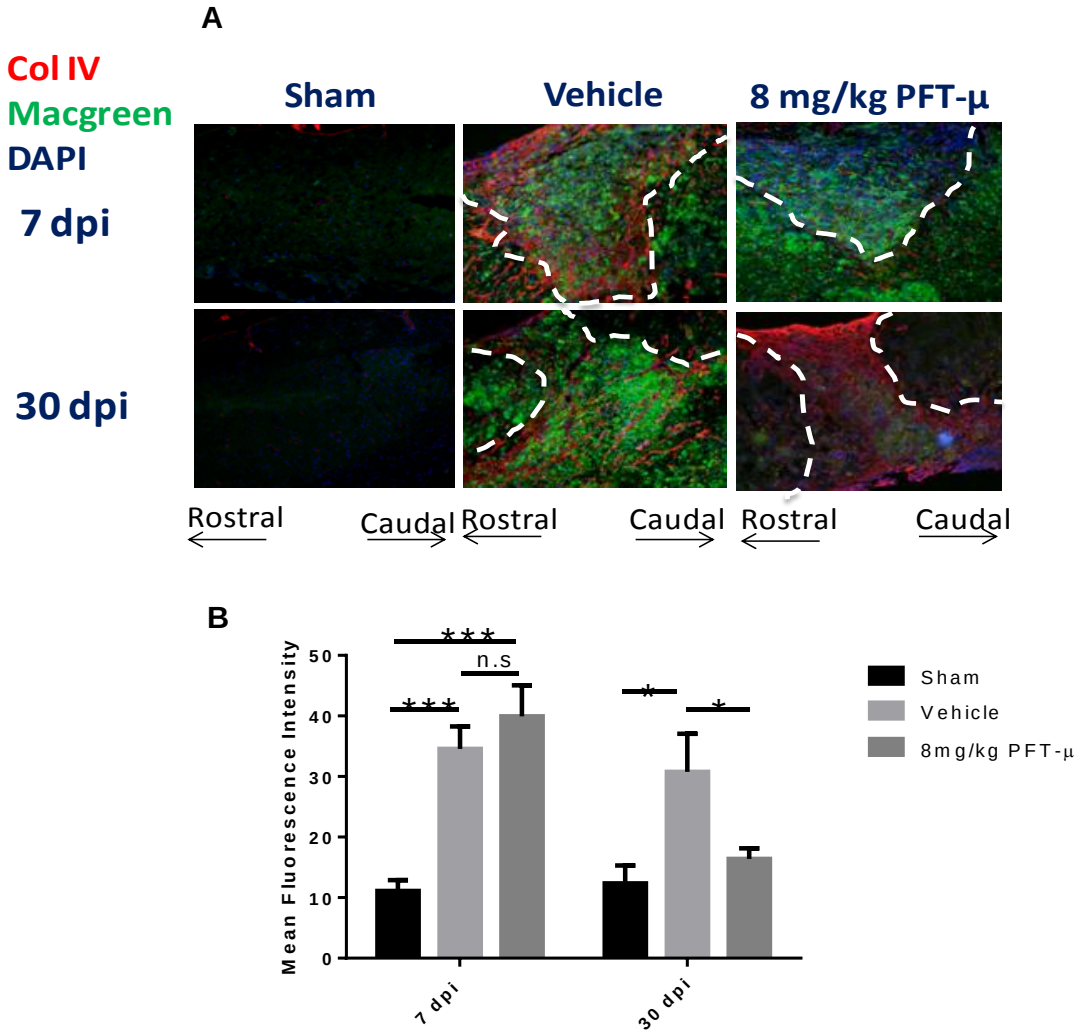

Figure 3-V: PFT-µ significantly reduces the presence of microglia/macrophages in the lesion site at 30 days post injury. (A) Tissue sections from injured MacGreen mice were immunofluorescently labeled with an anti-Collagen IV antibody to delineate the lesion border. **(B)** The intensity of E-GFP signal contained within the lesion site was quantified by an observer blind to the treatment group using ImageJ. Sham controls underwent laminectomy without contusion. n=3-6 per group .Data are shown as mean ± SEM. *p<0.05, *** p<0.001

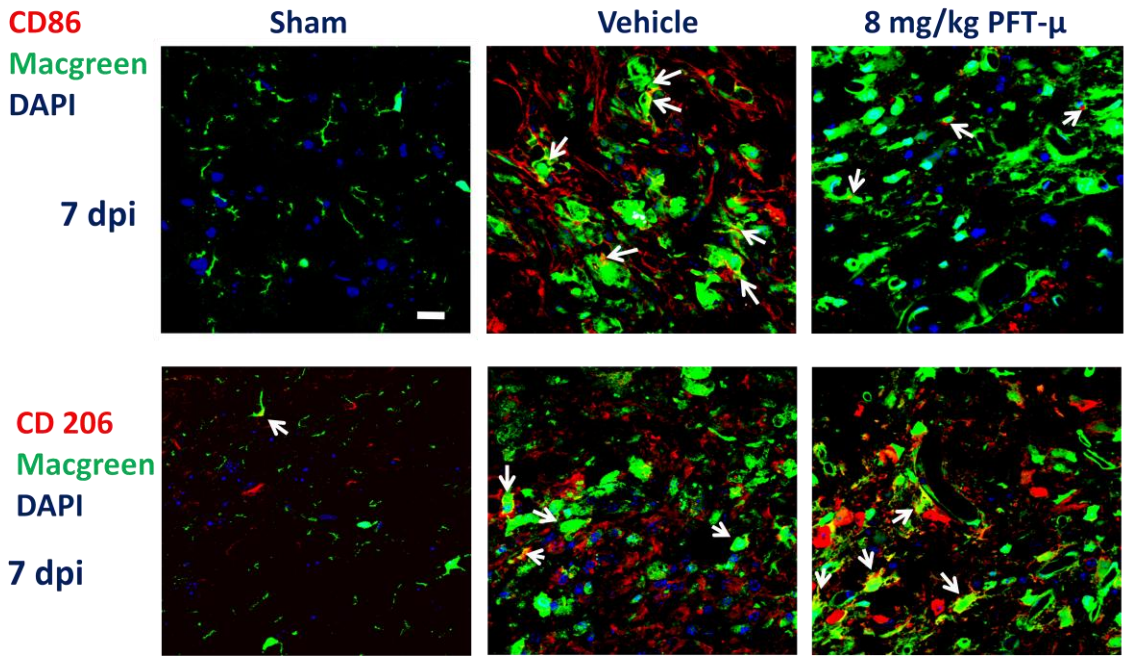

Figure 3-VI: PFT-µ reduces expression of M1 marker CD 86. Representative images from tissue sections from injured Macgreen mice immunofluorescently labeled with CD86 (top) or CD206 (bottom). Images were taken of microglia/macrophages present within the injury site. Six images were taken per section and five sections were imaged per biological replicate. White arrows point to double positive cells. Scale = 20 µm. n=3 per group

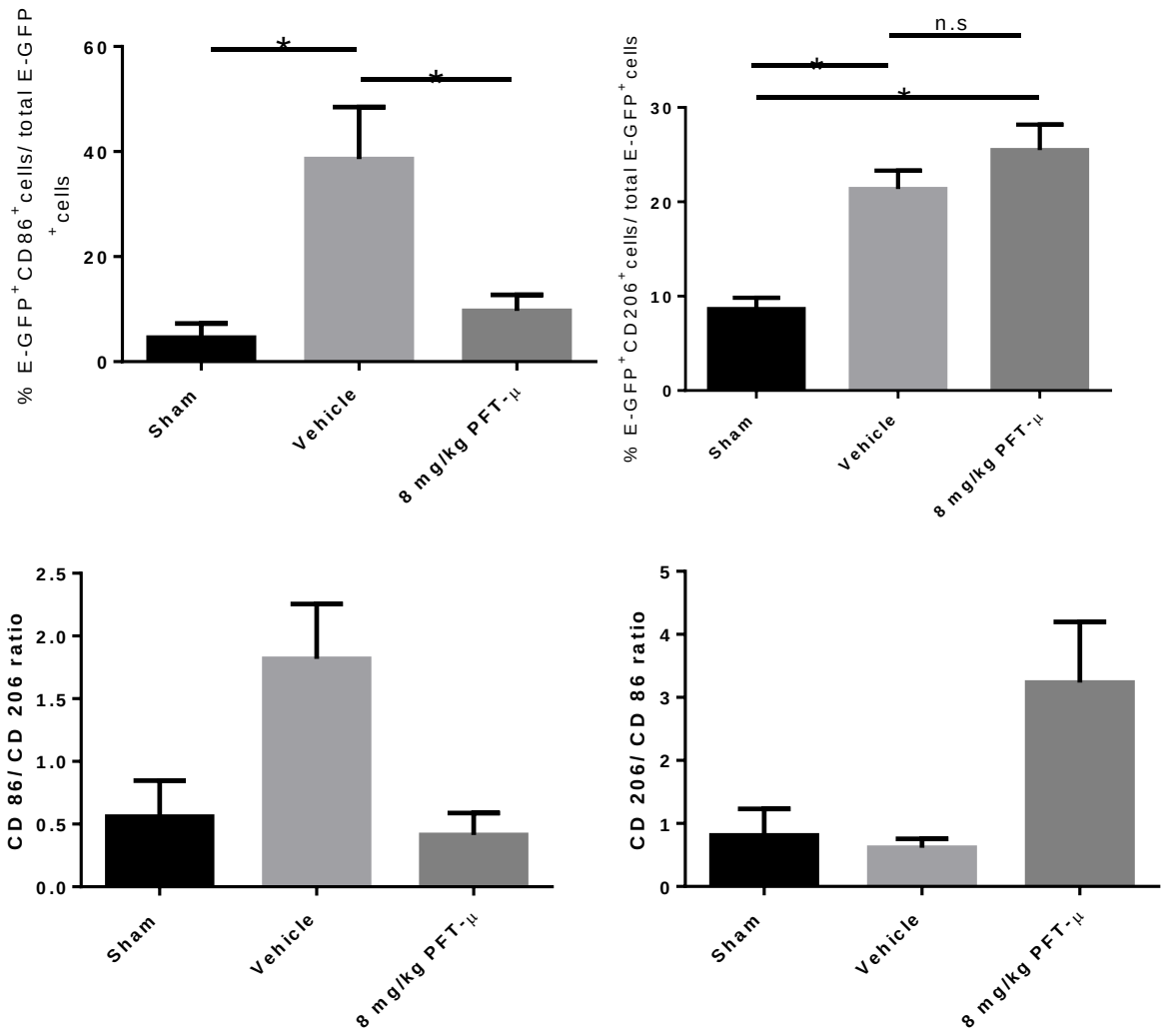

Figure 3-VII: PFT-μ significantly reduces expression of M1 marker CD86. Top: Quantification of the percentage of microglia/macrophages positive for expression of CD86 and CD206. **Bottom**: the data from the top graphs are shown as ratios. The ratio of CD86+ to $CD206^+$ microglia/macrophages and the ratio of $CD206^+$ to $CD86^+$ microglia/macrophages are shown. n=3 per group

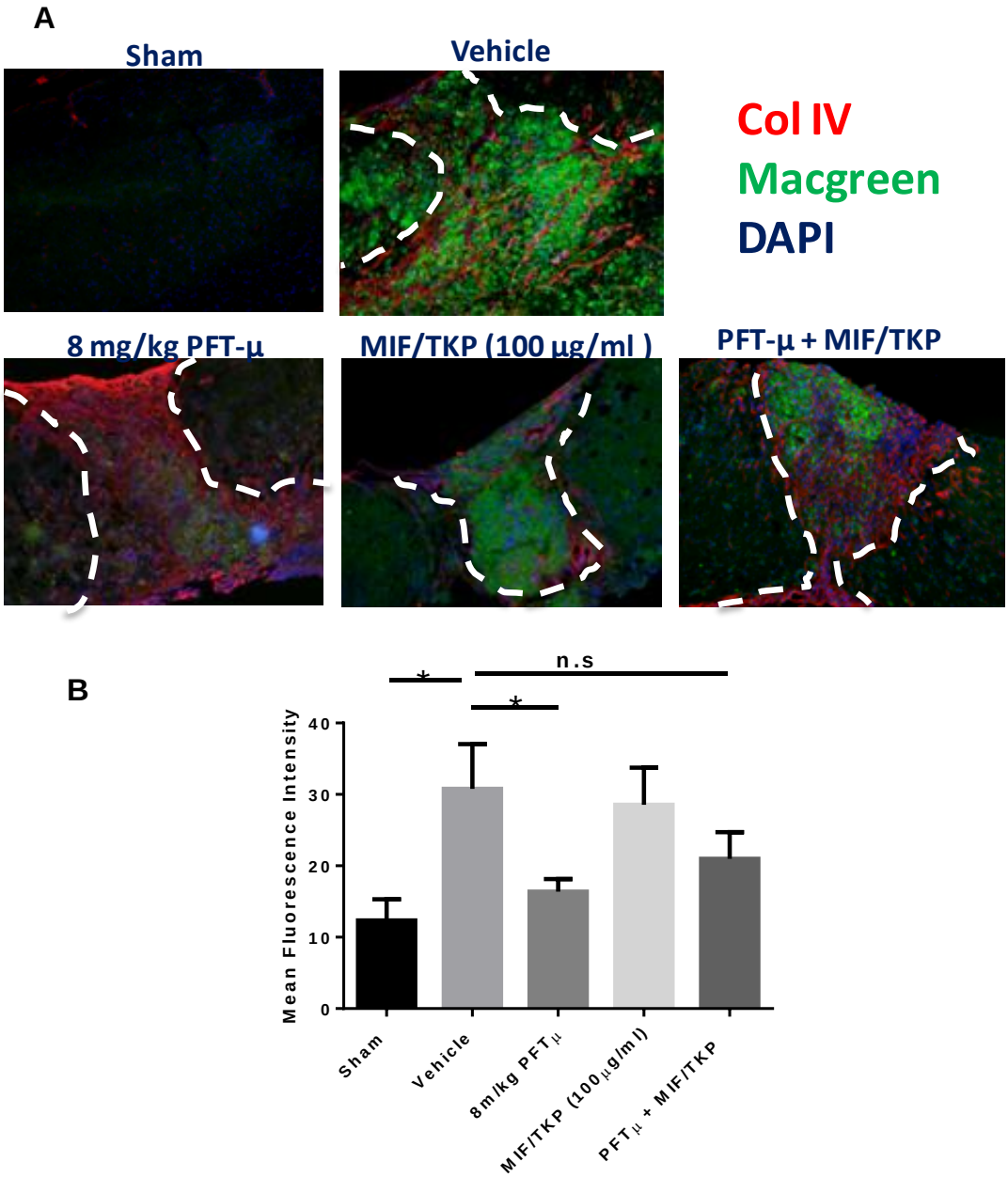

Figure 3-VIII: PFT-µ does not reduce the presence of microglia/macrophages in the lesion site when combined with MIF/TKP. (A) Tissue sections from injured MacGreen mice were immunofluorescently labeled with an anti-Collagen IV antibody to delineate the lesion border. **(B)** The intensity of E-GFP signal contained within the lesion site was quantified by an observer blind to the treatment group using ImageJ. Sham controls underwent laminectomy without contusion. n=3-6 per group .Data are shown as mean ± SEM. *p<0.05

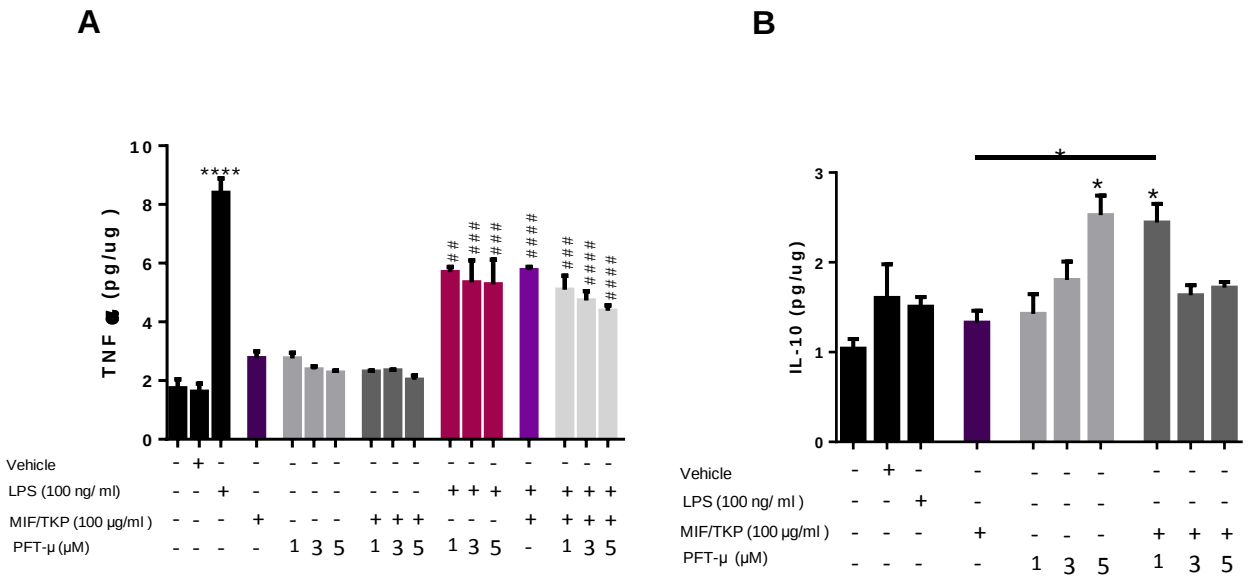

Figure 3-IX: PFT-µ reduces production of TNF-α and increases release of IL-10 in cultured microglia. TNF-α **(A)** and IL-10 levels **(B)** in conditioned media from cultured microglia were measured by ELISA. Data were normalized to total protein. Data are shown as mean ± SEM. *p<0.05, *** p<0.001**** p<0.0001

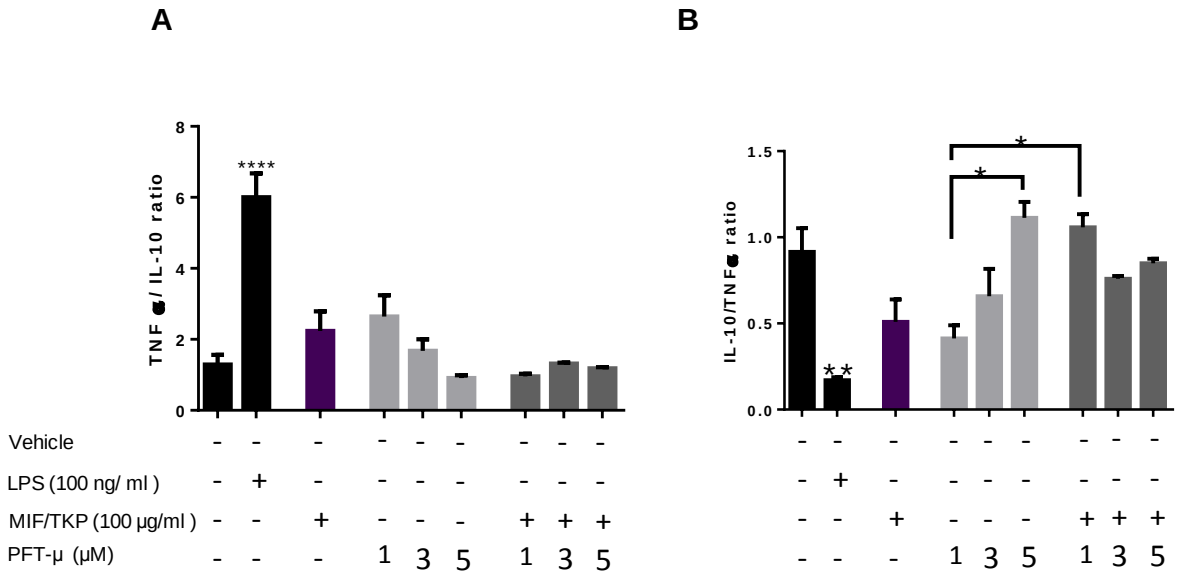

Figure 3-X: PFT-µ polarizes microglia to an M2 phenotype. TNF-α and IL-10 levels in conditioned media from cultured microglia were measured by ELISA. The ratio of TNF-α to IL-10 **(A)** and the ratio of IL-10 to TNF-α **(B)** were calculated. Data are shown as mean ± SEM. *p<0.05, **** p<0.0001

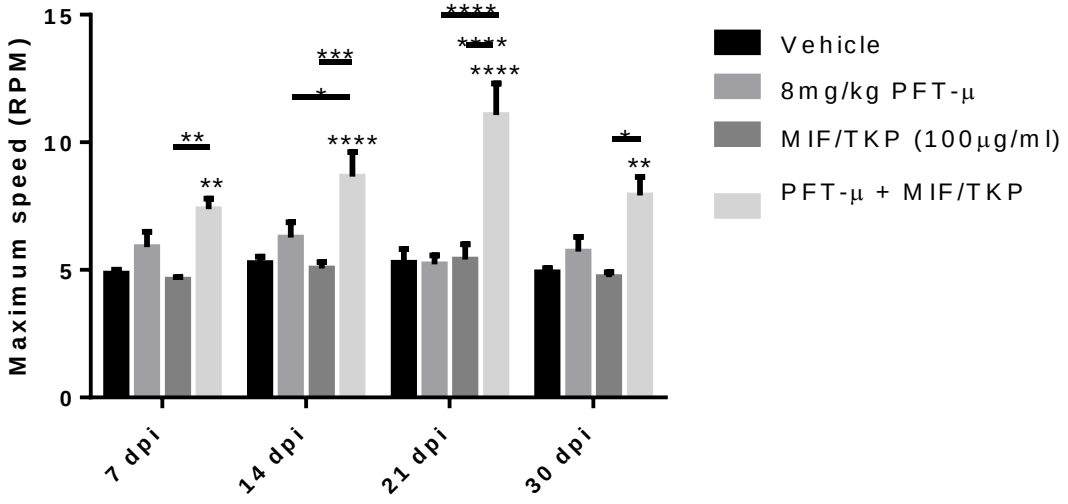

Figure 3-XI: PFT-μ significantly improves motor coordination and balance when combined with MIF/TKP. Injured mice were tested in the Rotarod at days 7, 14, 21, and 30 post SCI. n=3-15 per group Data are shown as mean ± SEM. *p<0.05, ** p<0.01, *** p<0.001, **** p<0.0001

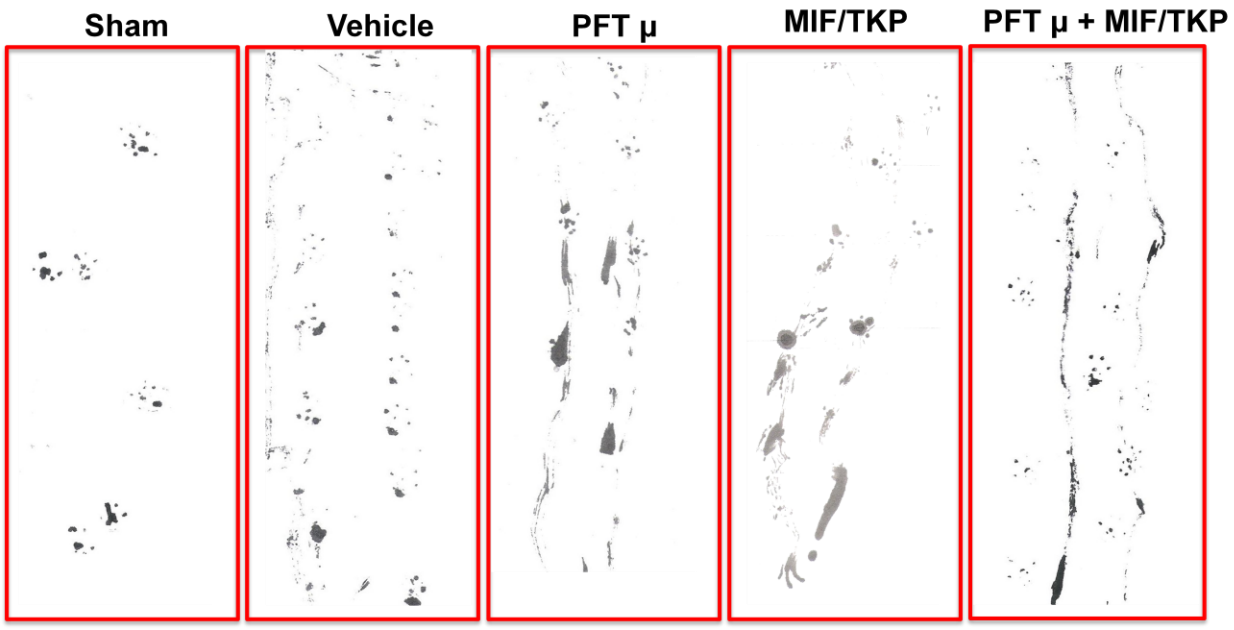

Figure 3-XII: PFT-μ significantly improves posture and gait when combined with MIF/TKP. Footprint analysis was conducted on days 7 and 30 post SCI. Representative images of footprints taken at 7 days post injury are shown. n=3-10 per group.

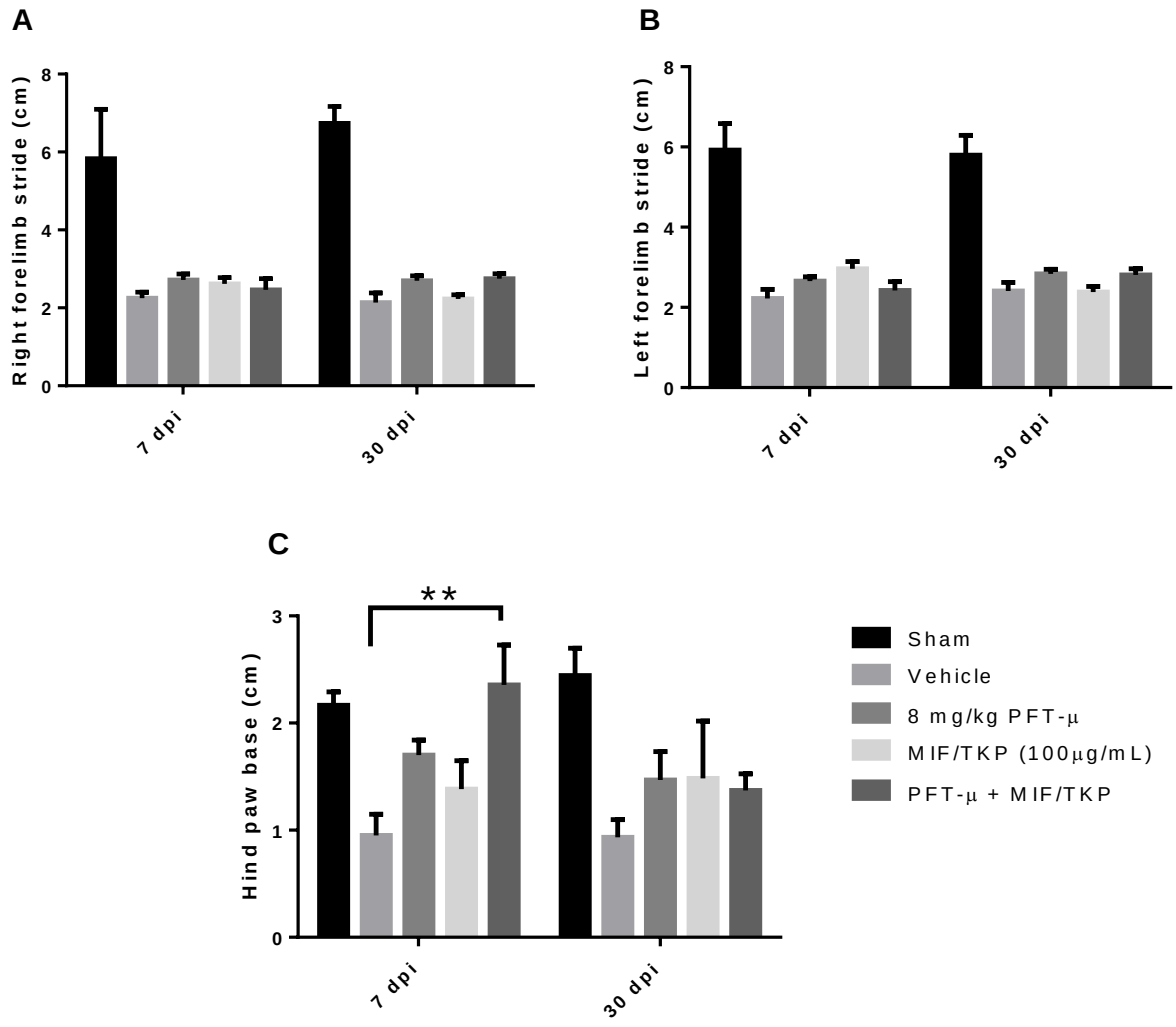

Figure 3-XIII: PFT-μ significantly improves posture and gait when combined with MIF/TKP. Footprint analysis was conducted on days 7 and 30 post SCI. **(A)** Right forelimb stride, **(B)** Left forelimb stride, **(C)** Hind paw base. n=3-10 per group Data are shown as mean ± SEM. ** $p<0.01$

Chapter 4: A role for microglia in spatial learning and social behavior

Besides being active players in inflammation, microglia have an important supporting role in CNS maintenance and function, including modulation of neuronal activity. During early neurogenesis microglia phagocytose apoptotic cells and eliminate unwanted neuronal projections [7, 11]. They also control production of cortical neurons by regulating the proliferation and survival of neural precursor cells [12-17]. Microglia provide trophic support for the formation of neuronal circuits and are indispensible for neuronal survival [8]. Microglia directly modulate synaptic activity by contacting synapses in a CR3/C3-dependent manner [7, 11, 18]. In co-cultures of neurons and microglia, microglia eliminate synapses via phagocytosis [11]. Neuronal stimulation results in extension of microglial processes towards highly active neurons, which in turn reduces neuronal activity [19].

In the previous chapter I examined the role of microglia in the context of a pathological setting and how the microglia response can be modulated to improve functional recovery after spinal cord injury. In this chapter, I investigate the in vivo functional significance of microglia depletion in the healthy brain via two independent methods using an array of behavioral tests. I show that depleting microglia locally in the hippocampus using clodronate results in alterations in spatial memory and social behavior. Systemic depletion of microglia via Csf-1R inhibition transiently alters spatial memory but does not affect sociability. Replenishment of microglia reverses these effects, indicating a dynamic role for these cells in the regulation of such behaviors.

Hippocampal depletion of Iba-1$^+$ microglia in vivo results in alterations in spatial learning and sociability

Previous work from our lab showed an increase in excitatory postsynaptic currents in hippocampal slices in which microglia had been depleted using clodronate [163]. This increase in current was reversed when microglia were replenished. Addition of microglia to cultured neurons decreased synaptic activity compared to cultured neurons alone. This reduction in synaptic activity correlated with a reduction in the density of synapses, spine numbers, and expression of synaptic adhesion molecules such as protocadherin and SynCAM1, indicating that microglia play a role in the regulation of neuronal activity in the healthy brain by affecting the number of active synapses [163].

I set out to determine whether there were measurable functional outcomes of microglia depletion. I hypothesized that our ex vivo observations will be replicated in vivo, and may modify animal behavior. In initial experiments I investigated whether clodronate depletes microglia in vivo: Mice were given a single clodronate injection into only the right hemisphere of the CA1 hippocampus. Mice were euthanized at days 1- 7 post injection and the tissue was analyzed for the presence of microglia using the microglia marker Iba-1. Microglia depletion became apparent starting at day 1 after the injection of clodronate and continued up to day 5 (Figure 6-I). By day 7 microglia started to reappear. I also examined the sections histologically to examine neuronal viability (using cresyl violet stain) and the viability of astrocytes (using GFAP immunofluorescence). No differences were obvious between control and depleted tissue (Figure 6-I).

Once I confirmed the ability of clodronate to deplete microglia in vivo, mice were given a bilateral clodronate injection into the CA1 hippocampus and euthanized 5 days later. Iba-1$^+$

microglia were undetectable in the CA1 hippocampus of clodronate-treated animals (Figure 6-II, top panel), while $GFAP^+$ astrocytes were clearly visible throughout the brain (Figure 6-II, bottom panel). The viability of neurons was ascertained using cresyl violet staining (Figure 6-II, middle panel).

I tested the effect of microglia depletion on spatial learning and spatial exploration using Barnes maze, a hippocampus-dependent task [164]. Two to three month old wild-type male mice were given a bilateral dorsal hippocampal injection of clodronate and tested on the Barnes maze twice per day for five consecutive days. Testing sessions were separated by fifteen minutes and data from both sessions were averaged for analysis. Mice treated with clodronate found the location of the escape box more slowly compared to the saline controls (Figure 6-III, A), and this difference was significant at days 3 and 4 ($p = 0.04$ and $p= 0.03$, respectively). Consistent with a slower rate of learning, clodronate treated animals made significantly more visits to holes prior to entering the escape box compared to saline-treated mice at day 4 of testing (Figure 6-III,C. $p=0.01$). We found no difference in the time both groups took to enter the escape box (Figure 6-III, B). To assess whether hyperactivity or motor impairments in the injected animals were influencing the observed result, we assessed activity in an open field setup. Both clodronate- and saline-treated mice displayed similar numbers of photobeam breaks per session (Figure 6-III, D. $p=0.90$) and a similar number of total rearings per session (Figure 6-III, E. $p=0.57$).

The hippocampus has recently been identified as a critical area for social memory processing [165-167]. To determine whether hippocampal loss of microglia extended to social behavior, I used the Crawley's sociability and preference for social novelty test described in [129]. Saline-treated controls made significantly more active contacts ($p=0.03$) and spent more time with the cup containing a conspecific (stranger mouse 1) (Figure 6-IV, A. $p= 0.02$). Similarly, saline-

treated mice displayed a significant preference for the novel mouse (stranger mouse 2) (6-IV, B. p= 0.07 for number of active contacts, and p= 0.01 for duration of active contacts). Conversely, clodronate treated animals did not display a preference for either cup (Figure 6-IV, A-B. p= 0 .4061 and p =0.7537 for number of active contacts and duration of active contacts with stranger mouse 1, respectively. p= 0.7043 and p= 0.5217 for number of active contacts and duration of active contacts with stranger mouse 2, respectively). Subject mice spent a similar amount of time in both chambers, indicating equal exploration of the maze (Figure 6-IV, C. p=0.34 and p=0.44 for the saline-treated mice in sessions I and II, respectively. p=0.66 and p=0.22 for the clodronate-treated mice in sessions 1 and 2, respectively). The test was conducted for five consecutive days starting on day 1 after clodronate treatment, and differences were observed on day 2 of testing (Figure 6-IV). Together these results suggest a role for hippocampal microglia in spatial learning and social behavior.

The effect of microglia depletion on spatial memory and social behavior is reversed after Iba-1$^+$ cells repopulate the brain

To determine whether microglia are able to repopulate the hippocampus after discontinuation of clodronate treatment we performed a single bilateral clodronate injection into the CA1 hippocampus of wild-type mice and euthanized the animals at day 20 post treatment. This time point was chosen based on a previous report showing that microglia repopulate the brain of HSVTK mice within two weeks after ganciclovir treatment [168]. Figure 6-V shows that microglia fully repopulate the mouse hippocampus by day 20 after clodronate injection. The newly repopulated Iba1$^+$ cells do not differ morphologically or in numbers from the microglia in control brains. Astrocytes and neurons remained viable. To examine whether normal behavior would also return after microglial repopulation, mice were tested on the Barnes maze for five

consecutive days starting on day 20 after clodronate injection. On the last day of Barnes maze testing, open field activity and social behavior were quantified. Clodronate treated mice displayed similar latencies to find (Figure 6-VI, A. p=0.50 and p= 0.72 at days 3 and 4, respectively) and enter the escape box (Figure 6-VI, B) and made a similar number of hole visits compared to controls (Figure 6-VI, C. p=0.33). This is in contrast to days 3 and 4 where microglia-depleted mice displayed a significant delay in spatial learning (Figure 6-III). Activity levels between treated and control animals remained the same even after microglial repopulation (Figure 6-VI, D-E. p=0.8933 for total beam breaks and p=0.08 for total rearings). Clodronate treated animals showed effectively normal social behavior after repopulation by microglia (Figure 6-VII. p=0.004 for number of active contacts in the saline treated mice during session II, and p=0.0001 for duration of active contacts in clodronate treated animals during session II). Subject mice spent a similar amount of time in both chambers during Session I, indicating equal exploration of the maze (Figure 6-VII, C. p=0.33 and p=0.38 for the saline and clodronate treated mice in session I, respectively). During session II the control mice spent significantly more time in the chamber containing stranger mouse 2 (6-VII, C p=0.02), and clodronate treated animals displayed a similar tendency (p=0.53).

Systemic Csf1-R inhibition depletes Iba-1^{+} cells in the brain within 7 days and recapitulates the alterations in spatial memory observed with clodronate treatment. However, Csf1-R inhibition does not affect social behavior

To extend the findings from the local intrahippocampal injection studies, I employed a second, systemic method of microglial depletion that takes advantage of their dependency on Csf1R signaling for their development and survival [3, 128, 169-171]. Csf-1 and its receptor Csf-1R are essential for microglial proliferation, differentiation, survival, migration, and chemotaxis;

and are also expressed by osteoclasts, macrophages, Langerhans cells, and cells of non-myeloid origin [172-176]. Mice that have a frame shift mutation in Csf-1 ($CSF1^{op/op}$ mice) produce non-functional Csf-1 and have a significant reduction in tissue macrophages but have close to normal numbers of Langerhans cells and microglia [2]. Lack of functional Csf-1 leads to developmental and sensory defects including abnormal neuronal function in the visual cortex, olfactory deficits, bone malformation, impaired tooth formation, and reproductive impairments [169, 170, 177, 178]. Many of these defects are resolved by application of macrophage- colony stimulating factor (M-CSF) or by overexpression of CSF-1 [169, 170, 179, 180]. On the other hand, Csf-1R-/- mice display severely reduced microglia numbers and have reduced brain size, increased proliferation and apoptosis of neuronal progenitors, and reduced neuronal differentiation [170, 171].

PLX3397, a Csf1R inhibitor, was added to food pellets at a concentration of 290 mg/kg of chow as previously described [128, 179]. This concentration exceeds the relevant clinical dose, as we aimed to achieve maximal reduction of microglia. Wild-type mice were fed PLX3397 or control chow for 7 days. Their brains were collected, sectioned, and immunofluorescently labeled for Iba-1, GFAP, and NeuN. Consistent with previous findings [128], Figure 6-VIII shows depletion of microglia 7 days after Csf1R inhibition (Figure 6-VIII, top). While neurons were preserved, astrocytes appeared to have thicker processes as well as higher intensity of GFAP immunostaining. This is consistent with previous reports showing increased protein levels of astrocytic proteins GFAP and S100β in mice treated with PLX3397 [128]. These results are also consistent with the higher expression of GFAP and the higher astrocytic density observed in mice lacking Csf1R [171].

To compare the behavioral effects I observed with clodronate treatment, another group of wild-type mice were fed with PLX3397- or control- chow for 7 days. Their spatial memory and sociability test performance were tested as above. Consistent with our previous results, PLX3397 treated animals took longer times to find the escape box at days 3 and 4 of testing (Figure 6-IX, A. p= 0.02 and p=0.01, respectively). No difference was found in the amount of time taken to enter the escape box (Figure 6-IX, B). PLX3397 treated animals also made significantly more hole visits prior to entering the escape box at day 4 (6-IX, C. p= 0.01). Both groups had similar numbers of photobeam breaks and total rearings (Figures 6-IX, D-E. p=0.1540 and p=0.2352, respectively), indicating that systemic loss of microglia did not produce profound widespread effects on motor abilities, general activity level, temperament, or other aspects of well-being in the mice that would be reflected in diminished activity and exploration of a novel environment. However, in contrast to the observations in mice given clodronate treatment, PLX3397 treated mice displayed normal social behavior in the Crawley's sociability and preference for social novelty test (Figure 6-X). In addition to making significantly more active contacts with stranger mouse 1 during session I (p=0.003 and p=0.03 for control and PLX3397 treated mice, respectively; p=0.0008 and p=0.008 for duration of active contacts during session I in control and PLX3397 treated mice, respectively) and with stranger mouse 2 during session II (p=0.002 and p=0.01 for control and PLX3397 treated mice, respectively. p=0.01 and p=0.002 for duration of active contacts during session II in co control and PLX3397 treated mice, respectively), both control and PLX3397 treated mice spent a similar amount of time in the chambers during Session I, indicating equal exploration of the maze (Figure 6-X,C, p=0.82 and p=0.30 for the control and PLX3397 treated mice in session I, respectively). During session II both control and

PLX3397 treated mice spent significantly more time in the chamber containing stranger mouse 2 (Figure 6-X, C p=0.02 and p=0.004, respectively).

Iba-1$^+$ microglia replenish the brain after discontinuation of Csf1-R inhibition which reverses the effect of microglia depletion on spatial memory

Another group of mice were fed PLX3397 or control chow for 7 days to deplete microglia. The mice were then returned to their normal diet for 14 days as previously described [128]. Brains from experimental and control groups were sectioned and immunofluorescently labeled for Iba-1, GFAP, and NeuN. Figure 6-XI shows complete replenishment of Iba-1$^+$microglia in the CA-1 hippocampus of PLX3397-treated mice. This new microglia population displays an activated morphology. Similarly, GFAP$^+$ astrocytes appear more numerous and reactive. NeuN$^+$ neurons remained comparable to the control treatments.

Another group of mice were treated as above and tested in the Barnes maze and in the open field at day 14 after discontinuation of Csf1R inhibition. Control and PLX3397 treated mice had similar latencies to find the escape box (Figure 6-XII, A. p=0.27 and p= 0.33 for days 3 and 4, respectively). No differences were observed in the amount of time taken to enter the escape box (Figure 6-XII, B). Control mice made significantly more visits to holes prior to entering the escape box on day 2 (Figure 6-XII, C. p=0.007), consistent with a trend towards slightly higher activity levels in the open field test (Figure 6-XII, D-E. p=0.37 and p=0.78 for total photobeam breaks and rearings, respectively).

Discussion

In this study I used two methods of microglia depletion: Bilateral microinjections of clodronate in the dorsal hippocampus, and systemic inhibition of Csf1R. The first method provides anatomical specificity, allowing us to examine the functional consequences of loss of microglia in hippocampal-related behaviors. The second allowed us to compare the results to a method that produced more widespread effects. Clodronate is pinocytosed by microglia and metabolized by the cell into adenosine 5'- (beta, gamma-dichloromethylene) triphosphate, an ATP analog [181]. PLX3397 is an oral, selective tyrosine kinase inhibitor of CSF-1 that successfully crosses the blood-brain barrier [128]. Its ability to specifically target microglia and macrophages has allowed for its use in different disease models in which microglia and/or macrophages play a key role in disease progression. These include melanoma, astrocytoma, and pancreatic cancer [182-184].

In this study I show that microglia are dynamic modulators of performance in the Barnes maze, a spatial memory task. Both clodronate and PLX3397-treated animals showed normal levels of activity in the open field test. Therefore, anxiety-like behavior, hyper or hypo-activity, and motor defects can be eliminated as reasons underlying the altered spatial task performance. Furthermore, I found no difference in microglial density or morphology in the amygdala (the brain region that is important for fear and emotional responses) in clodronate-treated mice (data not shown). My results are consistent with other studies indicating a role for immune cells in learning and memory. Mice deficient in CNS-specific T cells exhibit deficits in spatial learning [185, 186], and immune deficiency in mice causes a spatial memory defect that can be rescued by immune reconstitution [187]. In a previous report Elmore *et al* (2014) showed that treatment with PLX3397 did not affect spatial memory as measured by Barnes maze. Spatial learning was

tested in the mice 3 weeks after administration of PLX3397, a much later time point than the one tested here. Although the configuration of the Barnes maze in my experiment is different than that in Elmore et al., 2014 a likely explanation could be that the alterations in spatial memory I observed at day 7 post Csf-1R inhibition are transient and there is compensation at later time points.

I also show social behavior alterations with local ablation of microglia via clodronate. This is in agreement with other studies that have linked reduced microglial density with reduced sociability [188, 189]. However, mice treated systemically display normal social behavior. This difference could be due to the fact that systemic microglia depletion compromises areas of the brain other than the hippocampus that have a role in the regulation of social behavior, such as the prefrontal cortex [190]. Inputs from the amygdala to the ventral hippocampus have also been shown to modulate social behavior[191]. The differences in social behavior were observed on day 2 post clodronate injection, a time point at which microglia are in the process of dying. The same social behavior test was conducted in mice with systemic microglia depletion on day 7 when most microglia were depleted, another reason that may account for the differences in social behavior.

I found that microglia can repopulate the brain, consistent with previous studies [128, 168]. In the case of clodronate treatment, repopulation by microglia reverses the alterations in spatial memory and social behavior, indicating an active role for microglia in regulating these behaviors. Withdrawal of the Csf-1R inhibitor reverses the effects on spatial memory. Microglial repopulation occurs from the proliferation and differentiation of $Nestin^{+}$ progenitors, rather than infiltration of circulating cells [128]. This is in agreement with studies that have shown the capacity of microglia to self-renew [192, 193].

Recent studies have linked low microglial density with behavioral disorders. Mice lacking the chemokine receptor CX3CR1 display a temporary reduction of microglia concomitant with deficient synaptic pruning and deficits in social behavior and spatial learning [189, 194]. Inducible CX3CR1 knockouts show reduced spine remodeling along with memory impairments in auditory-fear conditioning and object recognition [195]. Mice deficient in Fractalkine (CX3CL1), a chemokine that directs microglia towards developing synapses [196], reduces performance in contextual fear conditioning and cued fear conditioning [194]. Lack of microglial receptor CCR2 accelerates the appearance of memory deficits in models of Alzheimer's disease [197, 198]. Lastly, deletion of TNFα in hematopoietic cells results in reduced levels of chemokines in the maternal milk of mice, increasing hippocampal proliferation and improving spatial memory in the offspring [199].

In this study local microglia ablation led to behavior phenotypes that evoke comparison to several neuropsychiatric disorders. Postmortem studies have described reduced glia numbers, including astrocytes and oligodendrocytes, in cortical regions in depressed individuals [200-202]. Cancer or hepatitis C patients who receive therapy with immune stimulators such as IFN-α or IL-2, develop major depression [202]. Exposure to LPS leads to symptoms of depression in both healthy and experimental animals [203]. The anti-depressant effect of microglia stimulation was shown in a model of stress-induced depression in which numbers of microglia drastically decrease as the depression develops [204]. Microglia numbers went back to normal and the depression-like symptoms disappeared after treatment with GM-CSF.

Thus I show that microglia can dynamically modulate behaviors that are observed in neuropsychiatric disorders. Since we and others have previously shown that microglia can modify synaptic activity, these in vivo findings suggest that disruption of communication

between neurons and microglia contributes to these behavioral outcomes and represents a disturbance of normal CNS functioning.

Future directions

I have shown that local depletion of microglia using clodronate caused alterations in both learning and social behavior, and previous work showed that ablation of microglia via clodronate results in increases in neuronal activity [163]. These changes may be attributed to microglia specifically since these behaviors are reversed upon microglia replenishment. On the other hand, global microglia depletion using PLX3397 affected learning but not social behavior, contradicting a previous study that reported no change in spatial learning [128]. The effect of PLX3397 on spatial memory might only be transient as I have shown memory alterations after seven days of continuous treatment, while Elmore, *et al* observed no effect after three weeks. The effect of PLX3397 on neuronal activity and synaptic remodeling should be determined as more widespread depletion of microglia might have a different effect compared to local depletion. Possible compensatory mechanisms such as astrocytic input should be investigated given that astrocyte reactivity was observed after systemic depletion of microglia. It would be valuable to determine how astrocytic activity changes in response to loss of microglia and whether astrocytes can modulate synaptic activity independently of microglia.

The mechanism through which microglia affect learning and social behavior is not well defined. It has been suggested that microglia-derived BDNF has a role in memory consolidation and that glial cell loss correlates with depression-like behavior [195, 201, 205]. In light of what is known about modulation of synaptic activity by microglia, our findings suggest that disruption of communication between neurons and microglia contributes to these behavioral outcomes and

represents a disturbance of normal functioning. However, the input from other glial cells in the cross-talk between neurons and microglia should be investigated.

Further experiments are needed to determine how clodronate and PLX3397 treatments compare in terms of the extent of microglia depletion. Microglia numbers in the brain should be determined at different time points after treatment and correlated to both behavioral outcomes and neuronal excitability. This would help determine whether changes in behavior and synaptic plasticity occur concomitantly with changes in microglia numbers in the brain.

Another future direction is to determine why neuronal hyperexcitablity resulting from microglia depletion produces negative alterations in behavior. Neuronal hyperexcitability has been associated with aggressiveness and alterations in other types of social behavior [206], which is consistent with the observed effects of microglia depletion on sociability. It has been proposed that microglia impairments lead to reductions in learning-dependent synaptic formation which may explain the learning deficits observed with microglia depletion [195]. However, individuals with autism spectrum disorders, which are characterized by learning and social behavior impairments, display reduced neural activation in the amygdala and the prefrontal cortex compared to healthy controls [207]. Inactivation of pyramidal neurons in the CA3 hippocampus leads to deficits in social memory [165]. Mice lacking Cx3Cr1 have a transient reduction of microglia numbers, impairments in hippocampal-dependent tasks, reduced synaptic plasticity, and reduced connectivity between the prefrontal cortex and the dorsal hippocampus resulting in impaired social behavior [189]. A proteomic screen revealed that microglia depletion leads to changes in expression of several genes with known synaptic functions including the NMDA receptor subunit GluN2B and vesicular glutamate transporter 1 (VGluT1) [195]. The contribution of these proteins to the regulation of animal behaviors should be examined in order

to understand the possible mechanisms governing increases in neuronal activity and reduced performance in cognitive tasks.

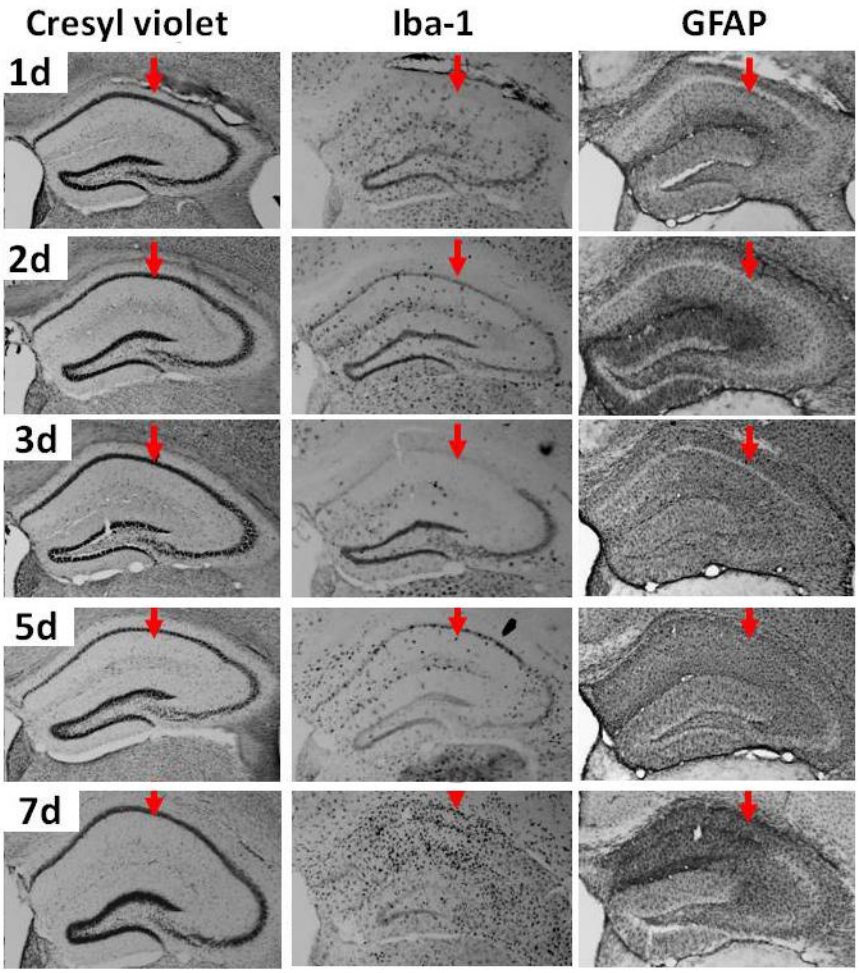

Figure 6-I: Clodronate depletes microglia in vivo. Wild-type mice were injected with clodronate in the right hemisphere of the CA1 hippocampus. Red arrows point to the injection site. Mice were euthanized at days 1-7 post injection and brain sections were stained for Cresyl violet (left panel), Iba-1 (middle panel), and GFAP (right panel). n=3 per group

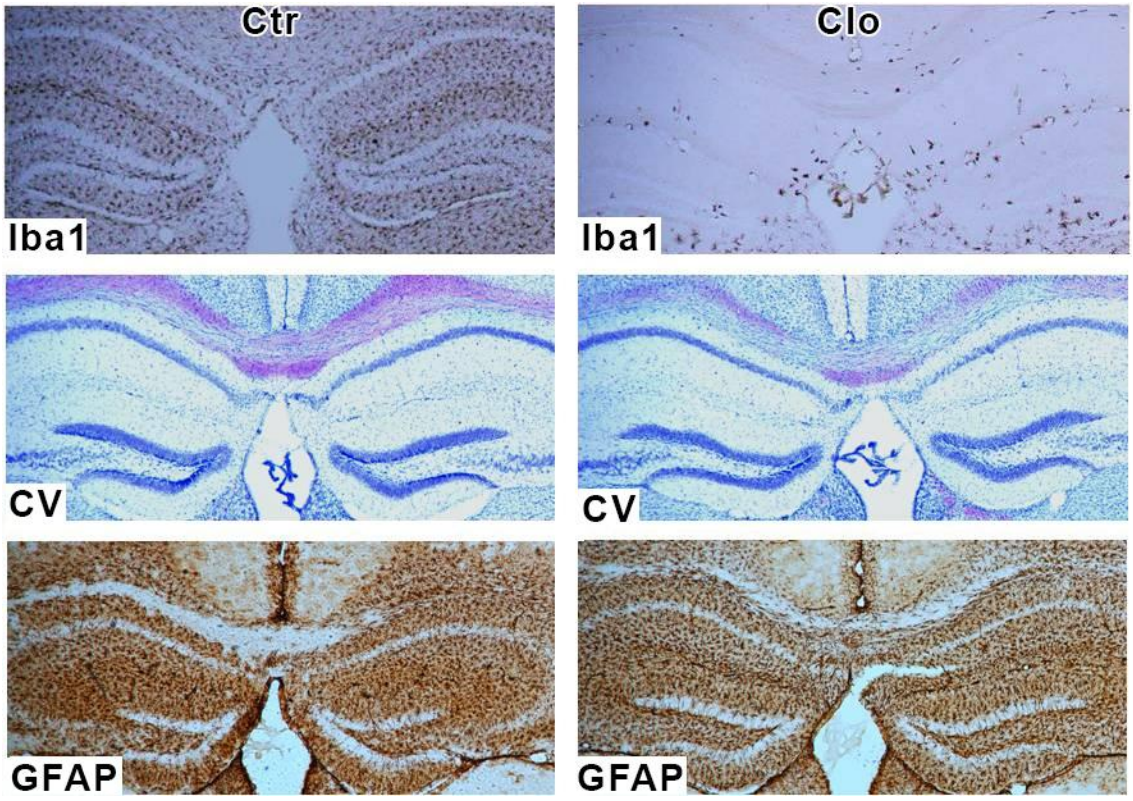

Figure 6-II: Hippocampal depletion of microglia by clodronate. Brain sections stained for Iba-1 (top panel), cresyl violet (middle panel), and GFAP (bottom panel) 5 days after clodronate injection into both brain hemispheres. n=9 per group.

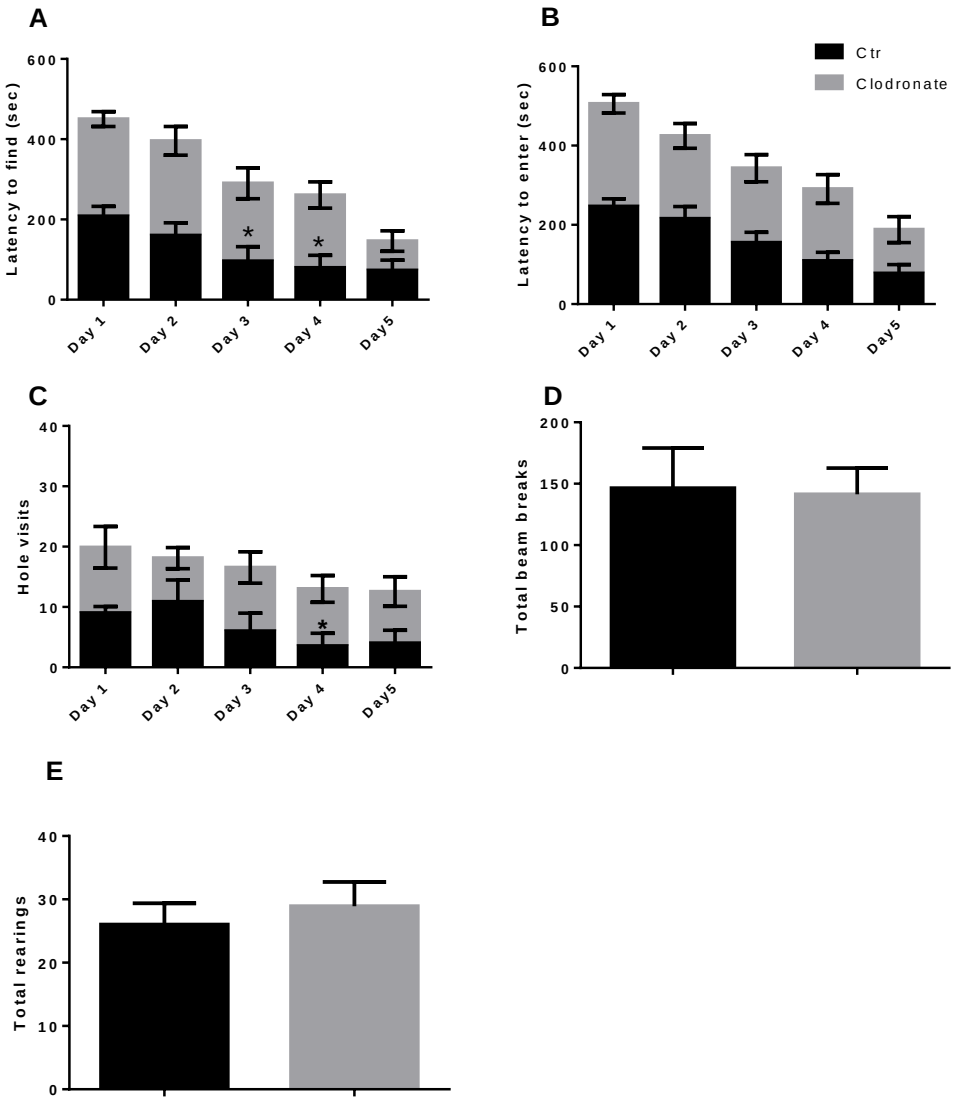

Figure 6-III: Hippocampal depletion of microglia by clodronate results in alterations in spatial learning. Mice were tested in the Barnes maze for five consecutive days starting at day 1 post clodronate injection. **(A)** Time taken to find the escape box (**B)** Time taken to enter the escape box. (**C)** Number of visits made to other holes before finding the escape box. n=9 per group. **(D-E)** The locomotor activity of the mice was assessed on day 5 after clodronate injection using the open field activity test. n=9-13 per group. Data are shown as mean ± SEM. *P<0.05

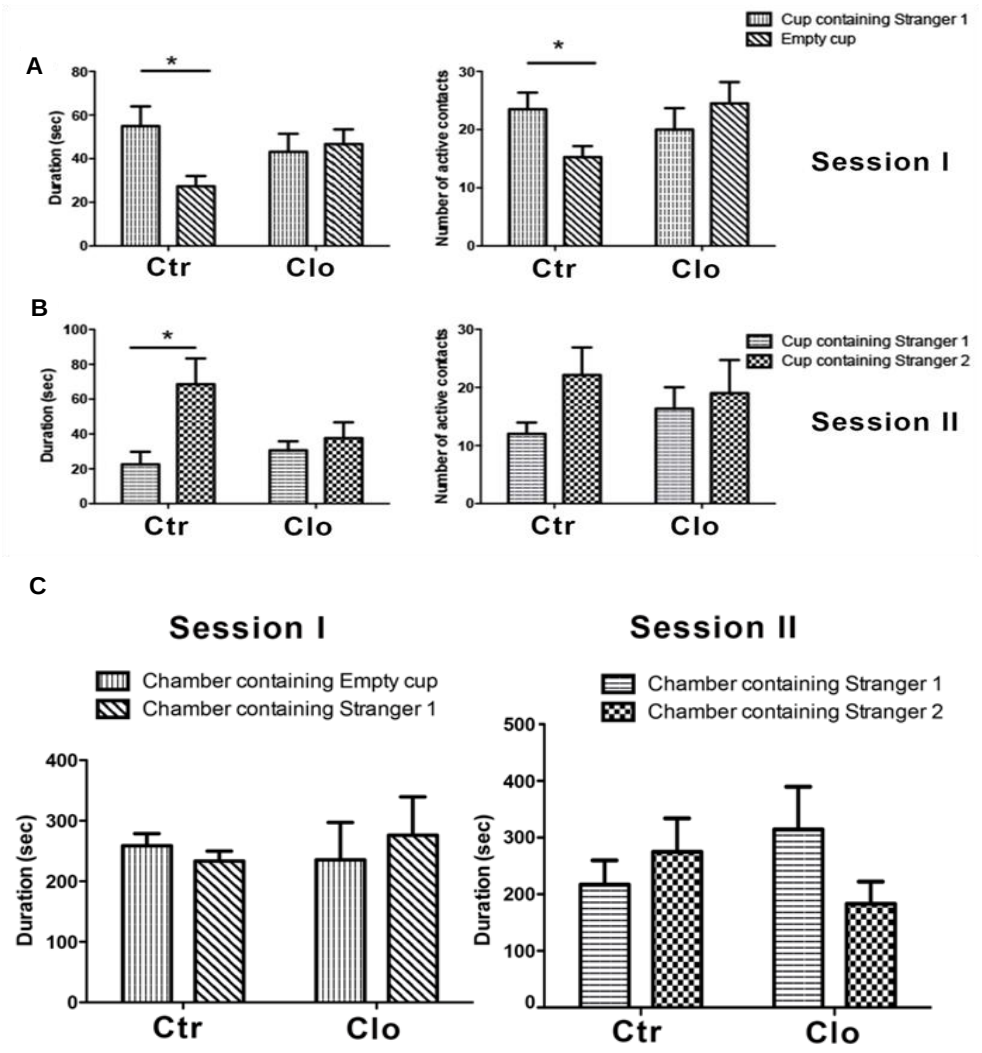

Figure 6-IV: Hippocampal depletion of microglia by clodronate results in alterations in social behavior. Mice were tested for five consecutive days on the Crawley's sociability and preference for social novelty test starting at day 1 post injection. Day 2 of testing is shown. (**A)** Duration and number of active contacts between subject mouse and stranger mouse 1 (Session I). (**B)** Duration and number of active contacts between subject mouse and stranger mouse 2 (Session II). (**C)** Time spent by subject mice in each chamber. n= 3-8 per group. Data are shown as mean ± SEM. *P<0.05

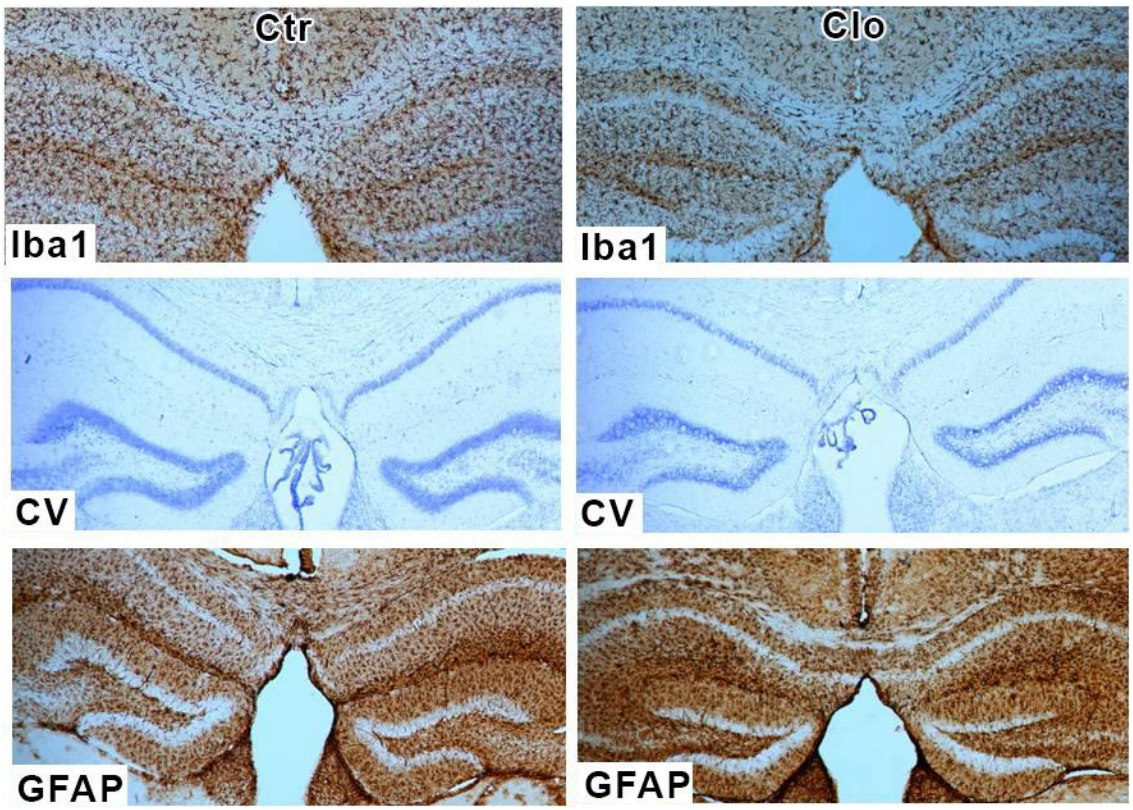

Figure 6-V: Repopulation of the hippocampus by microglia. Brain sections stained for Iba-1 (top panel), cresyl violet (middle panel), and GFAP (bottom panel) 20 days after clodronate injection. n=4 per group.

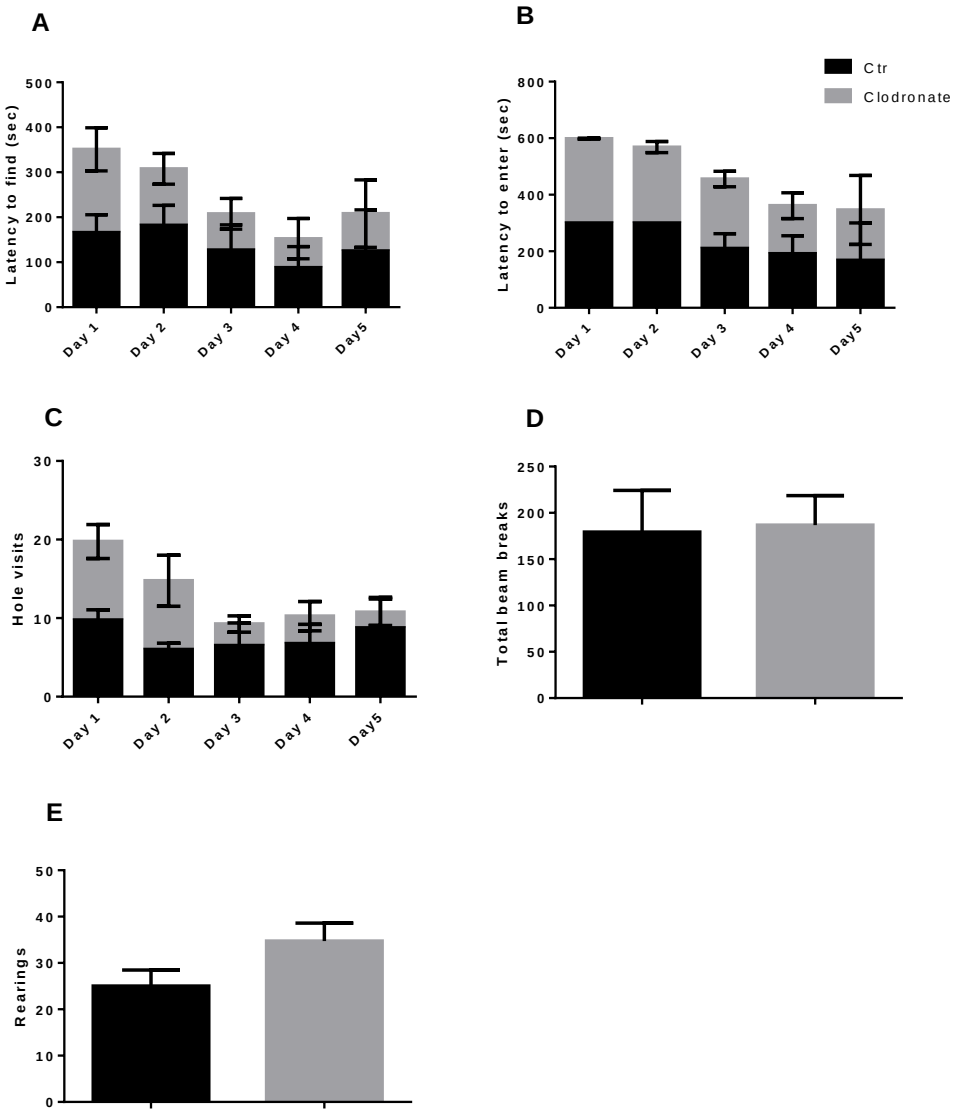

Figure 6-VI: Repopulation of the hippocampus by microglia reverses the effect on spatial memory. Mice were tested in the Barnes maze for five consecutive days starting at day 20 post clodronate injection. (A) Time taken by the mice to find the escape box. (**B)** Time taken by the mice to enter the escape box. (**C)** Number of visits made to other holes before finding the escape box. n=4 per group. **(D-E)** The locomotor activity of the mice was assessed on day 25 after clodronate injection using the open field activity test. n=4-7 per group. Data are shown as mean ± SEM.

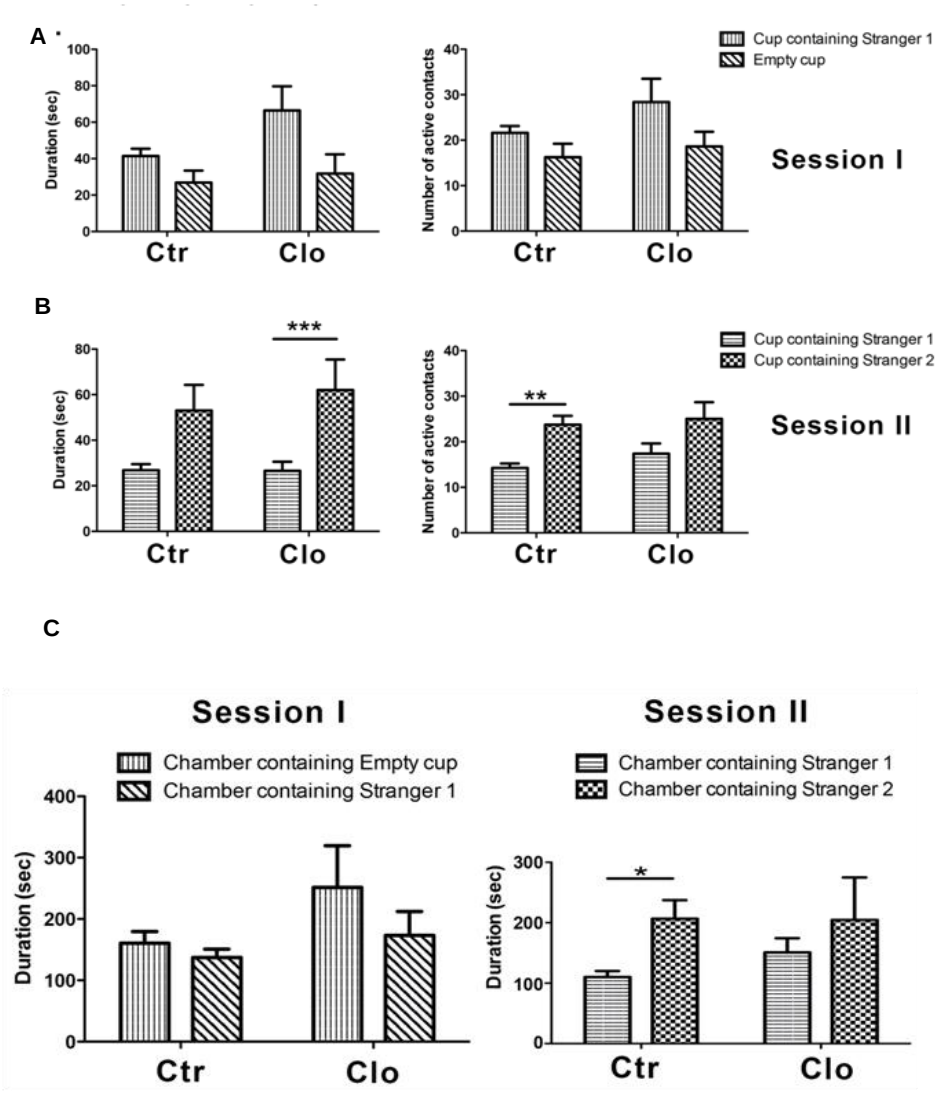

Figure 6-VII: Repopulation of the hippocampus by microglia reverses the effect on social behavior. Mice were tested on the Crawley's sociability and preference for social novelty test on day 25 after clodronate treatment. **(A)** Duration and number of active contacts between subject mouse and stranger mouse 1 (Session I). **(B)** Duration and number of active contacts between subject mouse and stranger mouse 2 (Session II). **(C)** Time spent by subject mice in each chamber. n= 3-8 per group. Data are shown as mean ± SEM. *P<0.05

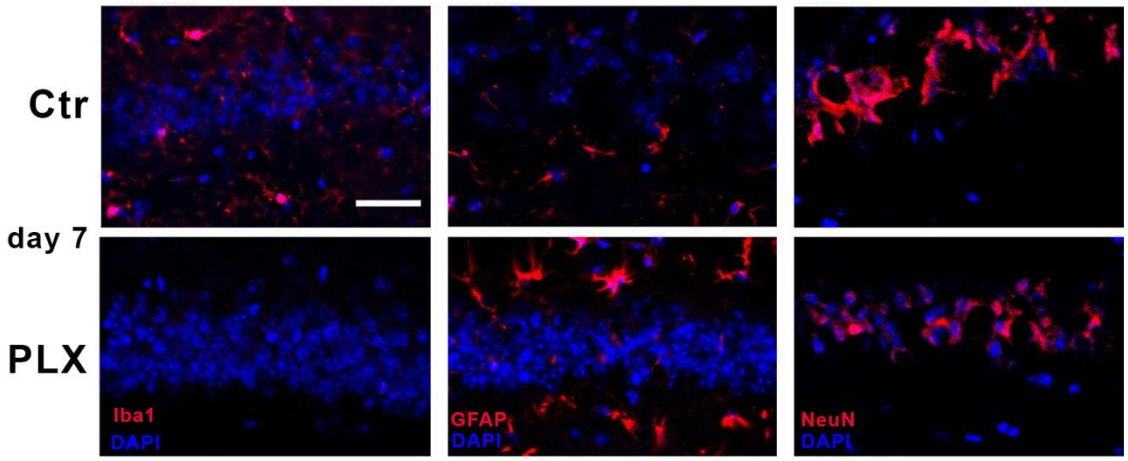

Figure 6-VIII. CSF1R inhibition via PLX3397 depletes microglia within 7 days. Wild-type mice were fed PLX3397 or control chow (AIN-76A) for 7 days. Brain sections were immunofluorescently labeled with anti- Iba-1 (left panel), anti-GFAP (middle panel), and anti-NeuN (right panel) n=3 per group. Scale = 50μm

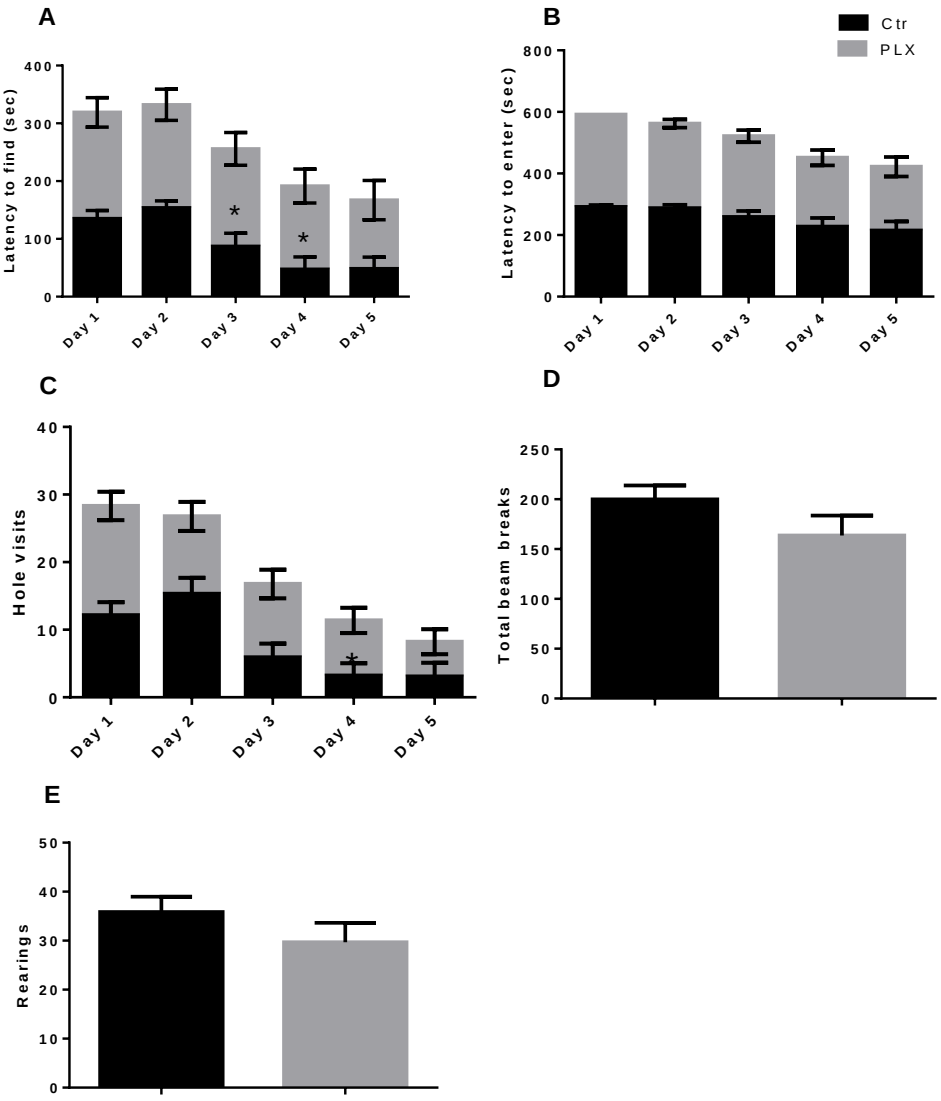

Figure 6-IX: Systemic microglia depletion recapitulates the effects on spatial memory observed with localized hippocampal depletion. Barnes maze test was conducted for 5 consecutive days one week after administration of PLX3397. **(A)** Time taken by the mice to find the escape box. (**B)**. Time taken by the mice to enter the escape box. (**C)** Number of visits made to other holes before finding the escape box. n=13 per. group. (**D-E**) The locomotor activity of the mice was assessed using the open field activity test on the last day of Barnes maze testing. n=13 per group. Data are shown as mean ± SEM. *p<0.05

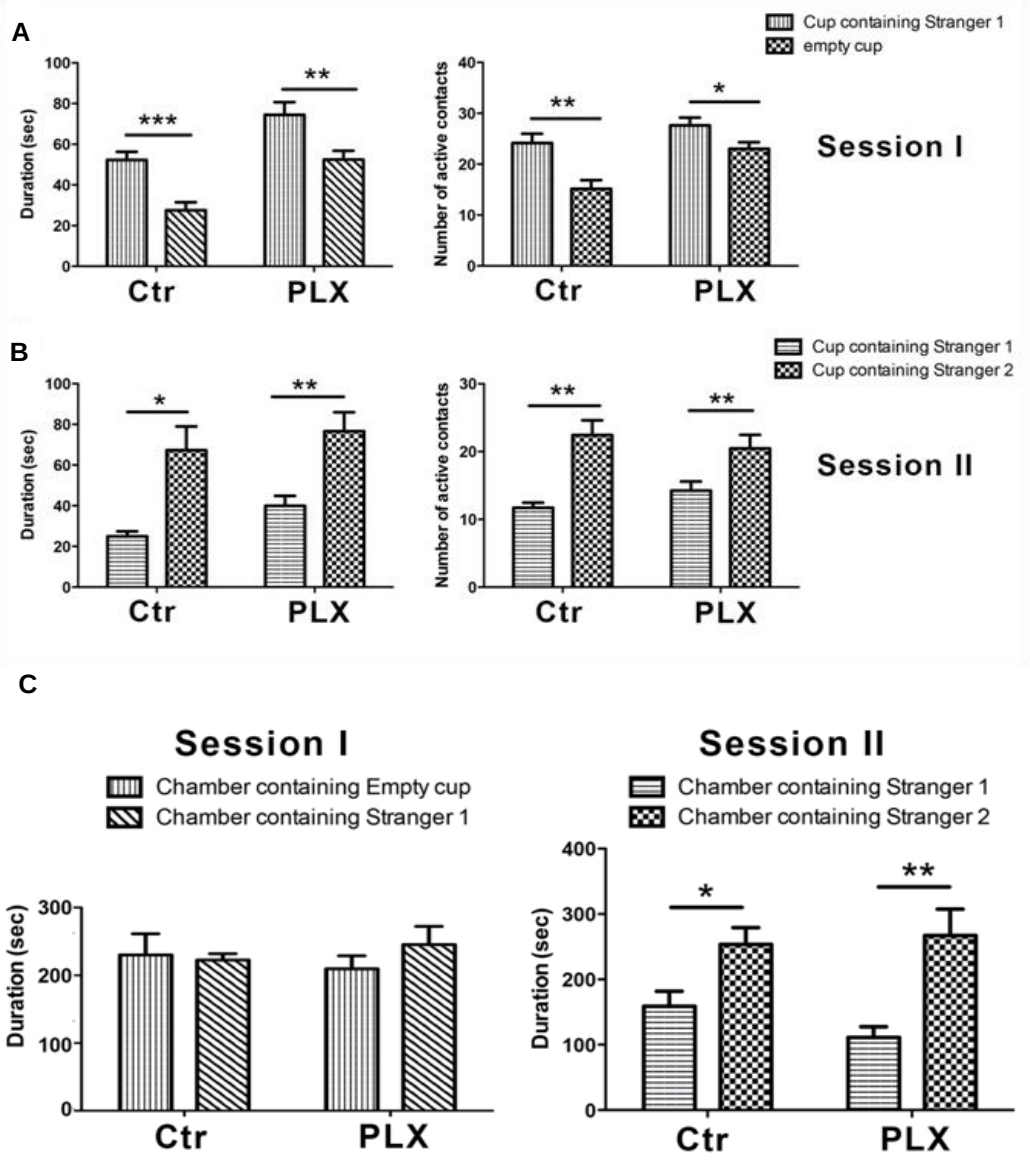

Figure 6-X: Social behavior is not affected by systemic microglia depletion. Social behavior was tested using the Crawleys's sociability and preference test on the last day of Barnes maze testing. **(A)** Duration and number of active contacts between subject mouse and stranger mouse 1 (Session I). (**B)** Duration and number of active contacts between subject mouse and stranger mouse 2 (Session II). (**C)** Time spent by subject mice in each chamber. n=7-13 per group. Data are shown as mean ± SEM. *p<0.05, ** p<0.01, *** p<0.001

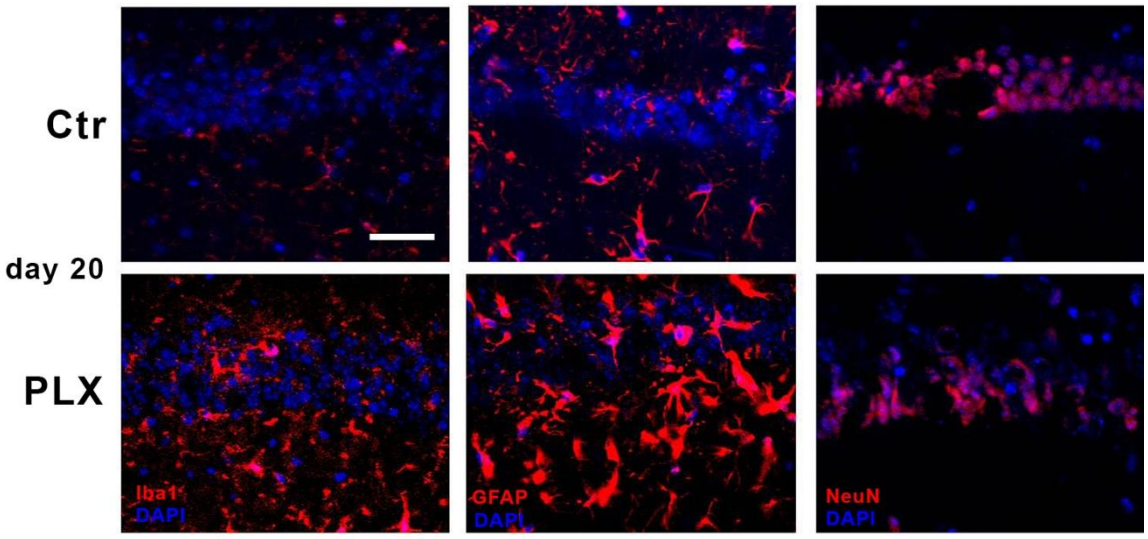

Figure 6-XI: Repopulation occurs within 14 days after withdrawal of PLX3397. Wild-type mice were fed PLX3397 or control chow (AIN-76A) for 7 days. Mice were then returned to their regular diet and euthanized two weeks after cessation of CSF1R inhibition. Brain sections were stained for Iba-1 (left panel), GFAP (middle panel), and NeuN (right panel) n=3 per group. Scale = 50μm

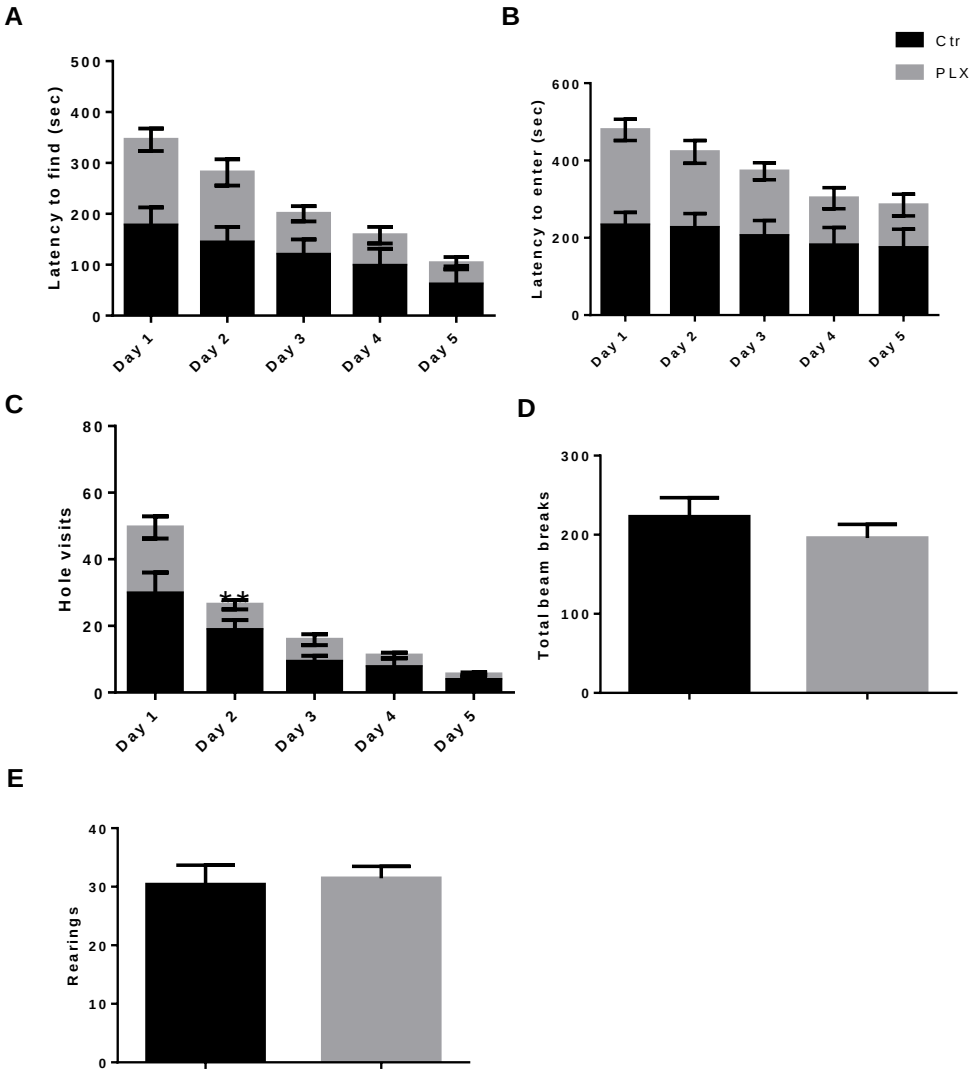

Figure 6-XII: Microglial repopulation of the brain reverses the performance in the Barnes maze. C57BL/6 mice were fed control or PLX3397-chow for 7 days. They were then returned to their regular diet for 14 days and tested on the Barnes maze. **(A)** Time taken by the mice to find the escape box. (**B)** Time taken by the mice to enter the escape box. (**C)** Number of visits made to other holes before finding the escape box. n=8-13 per group. (**D**-**E**) Locomotor activity was assessed using the open field activity test on the last day of Barnes maze testing. n=8-13 per group. Data are shown as mean ± SEM.

Thesis summary and future directions

Microglia are the first line of defense against disease in the CNS. They play key roles in several neurological diseases and can quickly respond to infection or injury [4, 5]. Under pathological conditions, microglia become activated and initiate an inflammatory response characterized by microglia proliferation and cytokine production[9]. However, their functions extend well beyond responding to activating stimuli. In the healthy CNS, microglia phagocytose apoptotic cells, prune synapses, and support the formation of neural circuits [7, 8]. Due to their extensive functions as supporting cells of the CNS, microglia are now considered active regulators of neurological function. In this work I have examined microglia in both pathological and physiological settings. In the contusion model of SCI microglial activation was attenuated by the use of a combination of drugs (PFT-μ and MIF/TKP) which resulted in smaller lesions and a significant improvement in motor function. In a parallel project, the effect of microglia depletion on cognitive and social abilities was examined using a variety of behavior tests. Lack of microglia was shown to affect spatial memory and social behavior. These effects were reversed once microglia were allowed to repopulate the brain, indicating an active role for microglia in the regulation of these behaviors as well as in disease progression during SCI.

The brain depends on immune cells, including microglia, for its maintenance and plasticity. Given that activation of microglia is common in many neurodegenerative diseases and given that microglia activation induces changes in gene expression, microglia activation may compromise the physiological function of microglia and contribute to disease progression. In future experiments the effect of the attenuation of microglial activation on oligodendrocyte survival, OPC proliferation, axonal growth, degradation of inhibitory molecules, and remyelination will be examined. Future work will also determine the mechanism through which microglia influence

learning and social behavior as well as the input from other glial cells in the cross-talk between neurons and microglia under steady-state conditions.

Bibliography

1. Kierdorf, K., et al., *Microglia emerge from erythromyeloid precursors via Pu.1- and Irf8-dependent pathways.* Nat Neurosci, 2013. **16**(3): p. 273-80.

2. Nayak, D., T.L. Roth, and D.B. McGavern, *Microglia development and function.* Annu Rev Immunol, 2014. **32**: p. 367-402.

3. Wegiel, J., et al., *Reduced number and altered morphology of microglial cells in colony stimulating factor-1-deficient osteopetrotic op/op mice.* Brain Res, 1998. **804**(1): p. 135-9.

4. Colton, C.A. and D.M. Wilcock, *Assessing activation states in microglia.* CNS Neurol Disord Drug Targets, 2010. **9**(2): p. 174-91.

5. Kraft, A.D. and G.J. Harry, *Features of microglia and neuroinflammation relevant to environmental exposure and neurotoxicity.* Int J Environ Res Public Health, 2011. **8**(7): p. 2980-3018.

6. Nimmerjahn, A., F. Kirchhoff, and F. Helmchen, *Resting microglial cells are highly dynamic surveillants of brain parenchyma in vivo.* Science, 2005. **308**(5726): p. 1314-8.

7. Paolicelli, R.C., et al., *Synaptic pruning by microglia is necessary for normal brain development.* Science, 2011. **333**(6048): p. 1456-8.

8. Ueno, M., et al., *Layer V cortical neurons require microglial support for survival during postnatal development.* Nat Neurosci, 2013. **16**(5): p. 543-51.

9. Hanisch, U.K., *Microglia as a source and target of cytokines.* Glia, 2002. **40**(2): p. 140-55.

10. Schwartz, M., et al., *How do immune cells support and shape the brain in health, disease, and aging?* J Neurosci, 2013. **33**(45): p. 17587-96.

11. Schafer, D.P., et al., *Microglia sculpt postnatal neural circuits in an activity and complement-dependent manner.* Neuron, 2012. **74**(4): p. 691-705.

12. Cunningham, C., *Microglia and neurodegeneration: the role of systemic inflammation.* Glia, 2013. **61**(1): p. 71-90.

13. Monje, M.L., H. Toda, and T.D. Palmer, *Inflammatory blockade restores adult hippocampal neurogenesis.* Science, 2003. **302**(5651): p. 1760-5.

14. Aarum, J., et al., *Migration and differentiation of neural precursor cells can be directed by microglia.* Proc Natl Acad Sci U S A, 2003. **100**(26): p. 15983-8.

15. Deierborg, T., et al., *Brain injury activates microglia that induce neural stem cell proliferation ex vivo and promote differentiation of neurosphere-derived cells into neurons and oligodendrocytes.* Neuroscience, 2010. **171**(4): p. 1386-96.

16. Guadagno, J., et al., *Microglia-derived TNFalpha induces apoptosis in neural precursor cells via transcriptional activation of the Bcl-2 family member Puma.* Cell Death Dis, 2013. **4**: p. e538.

17. Sierra, A., et al., *Microglia shape adult hippocampal neurogenesis through apoptosis-coupled phagocytosis.* Cell Stem Cell, 2010. **7**(4): p. 483-95.

18. Wake, H., et al., *Resting microglia directly monitor the functional state of synapses in vivo and determine the fate of ischemic terminals.* J Neurosci, 2009. **29**(13): p. 3974-80.

19. Li, Y., et al., *Reciprocal regulation between resting microglial dynamics and neuronal activity in vivo.* Dev Cell, 2012. **23**(6): p. 1189-202.

20. Sekhon, L.H. and M.G. Fehlings, *Epidemiology, demographics, and pathophysiology of acute spinal cord injury.* Spine (Phila Pa 1976), 2001. **26**(24 Suppl): p. S2-12.

21. Fehlings, M.G. and R. Vawda, *Cellular treatments for spinal cord injury: the time is right for clinical trials.* Neurotherapeutics, 2011. **8**(4): p. 704-20.

22. Hitzig, S.L., et al., *Secondary health complications in an aging Canadian spinal cord injury sample.* Am J Phys Med Rehabil, 2008. **87**(7): p. 545-55.

23. Dijkers, M., T. Bryce, and J. Zanca, *Prevalence of chronic pain after traumatic spinal cord injury: a systematic review.* J Rehabil Res Dev, 2009. **46**(1): p. 13-29.

24. Elmelund, M., P.S. Oturai, and F. Biering-Sorensen, *50 years follow-up on plasma creatinine levels after spinal cord injury.* Spinal Cord, 2014. **52**(5): p. 368-72.

25. Osterthun, R., et al., *Causes of death following spinal cord injury during inpatient rehabilitation and the first five years after discharge. A Dutch cohort study.* Spinal Cord, 2014. **52**(6): p. 483-8.

26. Zhang, Z. and L. Liao, *Risk factors predicting upper urinary tract deterioration in patients with spinal cord injury: a prospective study.* Spinal Cord, 2014. **52**(6): p. 468-71.

27. Simard, J.M., et al., *MRI evidence that glibenclamide reduces acute lesion expansion in a rat model of spinal cord injury.* Spinal Cord, 2013. **51**(11): p. 823-7.

28. Liu, D., W. Thangnipon, and D.J. McAdoo, *Excitatory amino acids rise to toxic levels upon impact injury to the rat spinal cord.* Brain Res, 1991. **547**(2): p. 344-8.

29. Panter, S.S., S.W. Yum, and A.I. Faden, *Alteration in extracellular amino acids after traumatic spinal cord injury.* Ann Neurol, 1990. **27**(1): p. 96-9.

30. Schwab, M.E. and D. Bartholdi, *Degeneration and regeneration of axons in the lesioned spinal cord.* Physiol Rev, 1996. **76**(2): p. 319-70.

31. Figley, S.A., et al., *Characterization of vascular disruption and blood-spinal cord barrier permeability following traumatic spinal cord injury.* J Neurotrauma, 2014. **31**(6): p. 541-52.

32. Hausmann, O.N., *Post-traumatic inflammation following spinal cord injury.* Spinal Cord, 2003. **41**(7): p. 369-78.

33. Grossman, S.D., L.J. Rosenberg, and J.R. Wrathall, *Temporal-spatial pattern of acute neuronal and glial loss after spinal cord contusion.* Exp Neurol, 2001. **168**(2): p. 273-82.

34. Stirling, D.P. and V.W. Yong, *Dynamics of the inflammatory response after murine spinal cord injury revealed by flow cytometry.* J Neurosci Res, 2008. **86**(9): p. 1944-58.

35. Beck, K.D., et al., *Quantitative analysis of cellular inflammation after traumatic spinal cord injury: evidence for a multiphasic inflammatory response in the acute to chronic environment.* Brain, 2010. **133**(Pt 2): p. 433-47.

36. David, S. and A. Kroner, *Repertoire of microglial and macrophage responses after spinal cord injury.* Nat Rev Neurosci, 2011. **12**(7): p. 388-99.

37. Fleming, J.C., et al., *The cellular inflammatory response in human spinal cords after injury.* Brain, 2006. **129**(Pt 12): p. 3249-69.

38. Gaudet, A.D. and P.G. Popovich, *Extracellular matrix regulation of inflammation in the healthy and injured spinal cord.* Exp Neurol, 2014. **258**: p. 24-34.

39. Jones, T.B., *Lymphocytes and autoimmunity after spinal cord injury.* Exp Neurol, 2014. **258**: p. 78-90.

40. Davalos, D., et al., *ATP mediates rapid microglial response to local brain injury in vivo.* Nat Neurosci, 2005. **8**(6): p. 752-8.

41. Colton, C.A., *Heterogeneity of microglial activation in the innate immune response in the brain.* J Neuroimmune Pharmacol, 2009. **4**(4): p. 399-418.

42. Pan, J.Z., et al., *Cytokine activity contributes to induction of inflammatory cytokine mRNAs in spinal cord following contusion.* J Neurosci Res, 2002. **68**(3): p. 315-22.

43. Rice, T., et al., *Characterization of the early neuroinflammation after spinal cord injury in mice.* J Neuropathol Exp Neurol, 2007. **66**(3): p. 184-95.

44. Carr, M.W., et al., *Monocyte chemoattractant protein 1 acts as a T-lymphocyte chemoattractant.* Proc Natl Acad Sci U S A, 1994. **91**(9): p. 3652-6.

45. Xu, L.L., et al., *Human recombinant monocyte chemotactic protein and other C-C chemokines bind and induce directional migration of dendritic cells in vitro.* J Leukoc Biol, 1996. **60**(3): p. 365-71.

46. Wolpe, S.D., et al., *Macrophages secrete a novel heparin-binding protein with inflammatory and neutrophil chemokinetic properties.* J Exp Med, 1988. **167**(2): p. 570-81.

47. Wolpe, S.D. and A. Cerami, *Macrophage inflammatory proteins 1 and 2: members of a novel superfamily of cytokines.* FASEB J, 1989. **3**(14): p. 2565-73.

48. Varnum, M.M. and T. Ikezu, *The classification of microglial activation phenotypes on neurodegeneration and regeneration in Alzheimer's disease brain.* Arch Immunol Ther Exp (Warsz), 2012. **60**(4): p. 251-66.

49. Colton, C. and D.M. Wilcock, *Assessing activation states in microglia.* CNS Neurol Disord Drug Targets, 2010. **9**(2): p. 174-91.

50. Kigerl, K.A., et al., *Identification of two distinct macrophage subsets with divergent effects causing either neurotoxicity or regeneration in the injured mouse spinal cord.* J Neurosci, 2009. **29**(43): p. 13435-44.

51. Miron, V.E., et al., *M2 microglia and macrophages drive oligodendrocyte differentiation during CNS remyelination.* Nat Neurosci, 2013. **16**(9): p. 1211-8.

52. Mosser, D.M. and J.P. Edwards, *Exploring the full spectrum of macrophage activation.* Nat Rev Immunol, 2008. **8**(12): p. 958-69.

53. Hu, X., et al., *Microglia/macrophage polarization dynamics reveal novel mechanism of injury expansion after focal cerebral ischemia.* Stroke, 2012. **43**(11): p. 3063-70.

54. Hawthorne, A.L. and P.G. Popovich, *Emerging concepts in myeloid cell biology after spinal cord injury.* Neurotherapeutics, 2011. **8**(2): p. 252-61.

55. Prineas, J.W., et al., *Immunopathology of secondary-progressive multiple sclerosis.* Ann Neurol, 2001. **50**(5): p. 646-57.

56. Gao, Z. and S.E. Tsirka, *Animal Models of MS Reveal Multiple Roles of Microglia in Disease Pathogenesis.* Neurol Res Int, 2011. **2011**: p. 383087.

57. Li, J., et al., *Tumor necrosis factor alpha mediates lipopolysaccharide-induced microglial toxicity to developing oligodendrocytes when astrocytes are present.* J Neurosci, 2008. **28**(20): p. 5321-30.

58. Pang, Y., Z. Cai, and P.G. Rhodes, *Disturbance of oligodendrocyte development, hypomyelination and white matter injury in the neonatal rat brain after intracerebral injection of lipopolysaccharide.* Brain Res Dev Brain Res, 2003. **140**(2): p. 205-14.

59. Buntinx, M., et al., *Cytokine-induced cell death in human oligodendroglial cell lines. II: Alterations in gene expression induced by interferon-gamma and tumor necrosis factor-alpha.* J Neurosci Res, 2004. **76**(6): p. 846-61.

60. Nicholas, R.S., et al., *Microglia-derived IGF-2 prevents TNFalpha induced death of mature oligodendrocytes in vitro.* J Neuroimmunol, 2002. **124**(1-2): p. 36-44.

61. Butovsky, O., et al., *Induction and blockage of oligodendrogenesis by differently activated microglia in an animal model of multiple sclerosis.* J Clin Invest, 2006. **116**(4): p. 905-15.

62. Pineau, I. and S. Lacroix, *Proinflammatory cytokine synthesis in the injured mouse spinal cord: multiphasic expression pattern and identification of the cell types involved.* J Comp Neurol, 2007. **500**(2): p. 267-85.

63. Bartholdi, D. and M.E. Schwab, *Expression of pro-inflammatory cytokine and chemokine mRNA upon experimental spinal cord injury in mouse: an in situ hybridization study.* Eur J Neurosci, 1997. **9**(7): p. 1422-38.

64. Gris, D., et al., *Transient blockade of the CD11d/CD18 integrin reduces secondary damage after spinal cord injury, improving sensory, autonomic, and motor function.* J Neurosci, 2004. **24**(16): p. 4043-51.

65. Emmetsberger, J. and S.E. Tsirka, *Microglial inhibitory factor (MIF/TKP) mitigates secondary damage following spinal cord injury.* Neurobiol Dis, 2012. **47**(3): p. 295-309.

66. Tan, A.M., et al., *Early microglial inhibition preemptively mitigates chronic pain development after experimental spinal cord injury.* J Rehabil Res Dev, 2009. **46**(1): p. 123-33.

67. Yang, L., et al., *Early expression and cellular localization of proinflammatory cytokines interleukin-1beta, interleukin-6, and tumor necrosis factor-alpha in human traumatic spinal cord injury.* Spine (Phila Pa 1976), 2004. **29**(9): p. 966-71.

68. Ferguson, A.R., et al., *Cell death after spinal cord injury is exacerbated by rapid TNF alpha-induced trafficking of GluR2-lacking AMPARs to the plasma membrane.* J Neurosci, 2008. **28**(44): p. 11391-400.

69. Rabchevsky, A.G. and W.J. Streit, *Grafting of cultured microglial cells into the lesioned spinal cord of adult rats enhances neurite outgrowth.* J Neurosci Res, 1997. **47**(1): p. 34-48.

70. McTigue, D.M. and R.B. Tripathi, *The life, death, and replacement of oligodendrocytes in the adult CNS.* J Neurochem, 2008. **107**(1): p. 1-19.

71. Karadottir, R., et al., *NMDA receptors are expressed in oligodendrocytes and activated in ischaemia.* Nature, 2005. **438**(7071): p. 1162-6.

72. Piani, D. and A. Fontana, *Involvement of the cystine transport system xc- in the macrophage-induced glutamate-dependent cytotoxicity to neurons.* J Immunol, 1994. **152**(7): p. 3578-85.

73. Domercq, M., et al., *System xc- and glutamate transporter inhibition mediates microglial toxicity to oligodendrocytes.* J Immunol, 2007. **178**(10): p. 6549-56.

74. Oyinbo, C.A., *Secondary injury mechanisms in traumatic spinal cord injury: a nugget of this multiply cascade.* Acta Neurobiol Exp (Wars), 2011. **71**(2): p. 281-99.

75. Rabchevsky, A.G., P.G. Sullivan, and S.W. Scheff, *Temporal-spatial dynamics in oligodendrocyte and glial progenitor cell numbers throughout ventrolateral white matter following contusion spinal cord injury.* Glia, 2007. **55**(8): p. 831-43.

76. Casha, S., W.R. Yu, and M.G. Fehlings, *Oligodendroglial apoptosis occurs along degenerating axons and is associated with FAS and p75 expression following spinal cord injury in the rat.* Neuroscience, 2001. **103**(1): p. 203-18.

77. Conforti, L., J. Gilley, and M.P. Coleman, *Wallerian degeneration: an emerging axon death pathway linking injury and disease.* Nat Rev Neurosci, 2014. **15**(6): p. 394-409.

78. Remington, L.T., et al., *Microglial recruitment, activation, and proliferation in response to primary demyelination.* Am J Pathol, 2007. **170**(5): p. 1713-24.

79. Clarner, T., et al., *Myelin debris regulates inflammatory responses in an experimental demyelination animal model and multiple sclerosis lesions.* Glia, 2012. **60**(10): p. 1468-80.

80. Shuman, S.L., J.C. Bresnahan, and M.S. Beattie, *Apoptosis of microglia and oligodendrocytes after spinal cord contusion in rats.* J Neurosci Res, 1997. **50**(5): p. 798-808.

81. Merrill, J.E., et al., *Microglial cell cytotoxicity of oligodendrocytes is mediated through nitric oxide.* J Immunol, 1993. **151**(4): p. 2132-41.

82. Yeo, Y.A., et al., *CD137 ligand activated microglia induces oligodendrocyte apoptosis via reactive oxygen species.* J Neuroinflammation, 2012. **9**: p. 173.

83. Li, J., et al., *Peroxynitrite generated by inducible nitric oxide synthase and NADPH oxidase mediates microglial toxicity to oligodendrocytes.* Proc Natl Acad Sci U S A, 2005. **102**(28): p. 9936-41.

84. Hamilton, S.P. and L.H. Rome, *Stimulation of in vitro myelin synthesis by microglia.* Glia, 1994. **11**(4): p. 326-35.

85. Baumann, N. and D. Pham-Dinh, *Biology of oligodendrocyte and myelin in the mammalian central nervous system.* Physiol Rev, 2001. **81**(2): p. 871-927.

86. Miller, R.H., *Regulation of oligodendrocyte development in the vertebrate CNS.* Prog Neurobiol, 2002. **67**(6): p. 451-67.

87. Noble, M., *Precursor cell transitions in oligodendrocyte development.* J Cell Biol, 2000. **148**(5): p. 839-42.

88. Totoiu, M.O. and H.S. Keirstead, *Spinal cord injury is accompanied by chronic progressive demyelination.* J Comp Neurol, 2005. **486**(4): p. 373-83.

89. Muramatsu, R., et al., *Angiogenesis induced by CNS inflammation promotes neuronal remodeling through vessel-derived prostacyclin.* Nat Med, 2012. **18**(11): p. 1658-64.

90. Liu, X.Z., et al., *Neuronal and glial apoptosis after traumatic spinal cord injury.* J Neurosci, 1997. **17**(14): p. 5395-406.

91. Beattie, M.S., Q. Li, and J.C. Bresnahan, *Cell death and plasticity after experimental spinal cord injury.* Prog Brain Res, 2000. **128**: p. 9-21.

92. Afshari, F.T., S. Kappagantula, and J.W. Fawcett, *Extrinsic and intrinsic factors controlling axonal regeneration after spinal cord injury.* Expert Rev Mol Med, 2009. **11**: p. e37.

93. Yong, V.W., et al., *Gamma-interferon promotes proliferation of adult human astrocytes in vitro and reactive gliosis in the adult mouse brain in vivo.* Proc Natl Acad Sci U S A, 1991. **88**(16): p. 7016-20.

94. Giulian, D., et al., *Interleukin-1 injected into mammalian brain stimulates astrogliosis and neovascularization.* J Neurosci, 1988. **8**(7): p. 2485-90.

95. Okada, S., et al., *Blockade of interleukin-6 receptor suppresses reactive astrogliosis and ameliorates functional recovery in experimental spinal cord injury.* J Neurosci Res, 2004. **76**(2): p. 265-76.

96. Silver, J. and J.H. Miller, *Regeneration beyond the glial scar.* Nat Rev Neurosci, 2004. **5**(2): p. 146-56.

97. Herrmann, J.E., et al., *STAT3 is a critical regulator of astrogliosis and scar formation after spinal cord injury.* J Neurosci, 2008. **28**(28): p. 7231-43.

98. Rodriguez, J.P., et al., *Abrogation of beta-catenin signaling in oligodendrocyte precursor cells reduces glial scarring and promotes axon regeneration after CNS injury.* J Neurosci, 2014. **34**(31): p. 10285-97.

99. Okada, S., et al., *Conditional ablation of Stat3 or Socs3 discloses a dual role for reactive astrocytes after spinal cord injury.* Nat Med, 2006. **12**(7): p. 829-34.

100. Cui, W., et al., *Inducible ablation of astrocytes shows that these cells are required for neuronal survival in the adult brain.* Glia, 2001. **34**(4): p. 272-82.

101. Schonberg, D.L., P.G. Popovich, and D.M. McTigue, *Oligodendrocyte generation is differentially influenced by toll-like receptor (TLR) 2 and TLR4-mediated intraspinal macrophage activation.* J Neuropathol Exp Neurol, 2007. **66**(12): p. 1124-35.

102. Talbott, J.F., et al., *Endogenous Nkx2.2+/Olig2+ oligodendrocyte precursor cells fail to remyelinate the demyelinated adult rat spinal cord in the absence of astrocytes.* Exp Neurol, 2005. **192**(1): p. 11-24.

103. Zeger, M., et al., *Insulin-like growth factor type 1 receptor signaling in the cells of oligodendrocyte lineage is required for normal in vivo oligodendrocyte development and myelination.* Glia, 2007. **55**(4): p. 400-11.

104. White, R.E. and L.B. Jakeman, *Don't fence me in: harnessing the beneficial roles of astrocytes for spinal cord repair.* Restor Neurol Neurosci, 2008. **26**(2-3): p. 197-214.

105. Moreno, M., et al., *Conditional ablation of astroglial CCL2 suppresses CNS accumulation of M1 macrophages and preserves axons in mice with MOG peptide EAE.* J Neurosci, 2014. **34**(24): p. 8175-85.

106. Chen, S.H., et al., *Microglial regulation of immunological and neuroprotective functions of astroglia.* Glia, 2015. **63**(1): p. 118-31.

107. Lau, L.W., et al., *Chondroitin sulfate proteoglycans in demyelinated lesions impair remyelination.* Ann Neurol, 2012. **72**(3): p. 419-32.

108. Rolls, A., R. Shechter, and M. Schwartz, *The bright side of the glial scar in CNS repair.* Nat Rev Neurosci, 2009. **10**(3): p. 235-41.

109. Smith-Thomas, L.C., et al., *An inhibitor of neurite outgrowth produced by astrocytes.* J Cell Sci, 1994. **107 (Pt 6)**: p. 1687-95.

110. McKeon, R.J., et al., *Reduction of neurite outgrowth in a model of glial scarring following CNS injury is correlated with the expression of inhibitory molecules on reactive astrocytes.* J Neurosci, 1991. **11**(11): p. 3398-411.

111. Davies, S.J., et al., *Regeneration of adult axons in white matter tracts of the central nervous system.* Nature, 1997. **390**(6661): p. 680-3.

112. Niederost, B.P., et al., *Bovine CNS myelin contains neurite growth-inhibitory activity associated with chondroitin sulfate proteoglycans.* J Neurosci, 1999. **19**(20): p. 8979-89.

113. Siebert, J.R., D.J. Stelzner, and D.J. Osterhout, *Chondroitinase treatment following spinal contusion injury increases migration of oligodendrocyte progenitor cells.* Exp Neurol, 2011. **231**(1): p. 19-29.

114. Siebert, J.R. and D.J. Osterhout, *The inhibitory effects of chondroitin sulfate proteoglycans on oligodendrocytes.* J Neurochem, 2011. **119**(1): p. 176-88.

115. Wang, D., et al., *Chondroitinase combined with rehabilitation promotes recovery of forelimb function in rats with chronic spinal cord injury.* J Neurosci, 2011. **31**(25): p. 9332-44.

116. Kanno, H., et al., *Combination of engineered Schwann cell grafts to secrete neurotrophin and chondroitinase promotes axonal regeneration and locomotion after spinal cord injury.* J Neurosci, 2014. **34**(5): p. 1838-55.

117. Bartus, K., et al., *Large-scale chondroitin sulfate proteoglycan digestion with chondroitinase gene therapy leads to reduced pathology and modulates macrophage phenotype following spinal cord contusion injury.* J Neurosci, 2014. **34**(14): p. 4822-36.

118. Ebert, S., et al., *Chondroitin sulfate disaccharide stimulates microglia to adopt a novel regulatory phenotype.* J Leukoc Biol, 2008. **84**(3): p. 736-40.

119. Rolls, A., et al., *Two faces of chondroitin sulfate proteoglycan in spinal cord repair: a role in microglia/macrophage activation.* PLoS Med, 2008. **5**(8): p. e171.

120. Brose, K. and M. Tessier-Lavigne, *Slit proteins: key regulators of axon guidance, axonal branching, and cell migration.* Curr Opin Neurobiol, 2000. **10**(1): p. 95-102.

121. Bukhari, N., et al., *Axonal Regrowth after Spinal Cord Injury via Chondroitinase and the Tissue Plasminogen Activator (tPA)/Plasmin System.* J Neurosci, 2011. **31**(42): p. 14931-43.

122. Auriault, C., et al., *Characterization and synthesis of a macrophage inhibitory peptide from the second constant domain of human immunoglobulin G.* FEBS Lett, 1983. **153**(1): p. 11-5.

123. Strom, E., et al., *Small-molecule inhibitor of p53 binding to mitochondria protects mice from gamma radiation.* Nat Chem Biol, 2006. **2**(9): p. 474-9.

124. Nijboer, C.H., et al., *Targeting the p53 pathway to protect the neonatal ischemic brain.* Ann Neurol, 2011. **70**(2): p. 255-64.

125. Bronstein, R., et al., *Culturing microglia from the neonatal and adult central nervous system.* J Vis Exp, 2013(78).

126. Carter, R.J., et al., *Characterization of progressive motor deficits in mice transgenic for the human Huntington's disease mutation.* J Neurosci, 1999. **19**(8): p. 3248-57.

127. Beastrom, N., et al., *mdx((5)cv) mice manifest more severe muscle dysfunction and diaphragm force deficits than do mdx Mice.* Am J Pathol, 2011. **179**(5): p. 2464-74.

128. Elmore, M.R., et al., *Colony-stimulating factor 1 receptor signaling is necessary for microglia viability, unmasking a microglia progenitor cell in the adult brain.* Neuron, 2014. **82**(2): p. 380-97.

129. Kaidanovich-Beilin, O., et al., *Assessment of social interaction behaviors.* J Vis Exp, 2011(48).

130. Sasmono, R.T., et al., *Mouse neutrophilic granulocytes express mRNA encoding the macrophage colony-stimulating factor receptor (CSF-1R) as well as many other macrophage-specific transcripts and can transdifferentiate into macrophages in vitro in response to CSF-1.* J Leukoc Biol, 2007. **82**(1): p. 111-23.

131. Soderblom, C., et al., *Perivascular fibroblasts form the fibrotic scar after contusive spinal cord injury.* J Neurosci, 2013. **33**(34): p. 13882-7.

132. Nakamura, Y., Q.S. Si, and K. Kataoka, *Lipopolysaccharide-induced microglial activation in culture: temporal profiles of morphological change and release of cytokines and nitric oxide.* Neurosci Res, 1999. **35**(2): p. 95-100.

133. Sedy, J., et al., *Methods for behavioral testing of spinal cord injured rats.* Neurosci Biobehav Rev, 2008. **32**(3): p. 550-80.

134. Schaar, K.L., M.M. Brenneman, and S.I. Savitz, *Functional assessments in the rodent stroke model.* Exp Transl Stroke Med, 2010. **2**(1): p. 13.

135. Hwang, D.H., et al., *Survival of neural stem cell grafts in the lesioned spinal cord is enhanced by a combination of treadmill locomotor training via insulin-like growth factor-1 signaling.* J Neurosci, 2014. **34**(38): p. 12788-800.

136. Balasingam, V. and V.W. Yong, *Attenuation of astroglial reactivity by interleukin-10.* J Neurosci, 1996. **16**(9): p. 2945-55.

137. Bethea, J.R., et al., *Systemically administered interleukin-10 reduces tumor necrosis factor-alpha production and significantly improves functional recovery following traumatic spinal cord injury in rats.* J Neurotrauma, 1999. **16**(10): p. 851-63.

138. Plunkett, J.A., et al., *Effects of interleukin-10 (IL-10) on pain behavior and gene expression following excitotoxic spinal cord injury in the rat.* Exp Neurol, 2001. **168**(1): p. 144-54.

139. Venna, V.R., et al., *Inhibition of mitochondrial p53 abolishes the detrimental effects of social isolation on ischemic brain injury.* Stroke, 2014. **45**(10): p. 3101-4.

140. Kotipatruni, R.R., et al., *p53- and Bax-mediated apoptosis in injured rat spinal cord.* Neurochem Res, 2011. **36**(11): p. 2063-74.

141. Saito, N., et al., *Implications of p53 protein expression in experimental spinal cord injury.* J Neurotrauma, 2000. **17**(2): p. 173-82.

142. Leu, J.I., et al., *A small molecule inhibitor of inducible heat shock protein 70.* Mol Cell, 2009. **36**(1): p. 15-27.

143. Mjahed, H., et al., *Heat shock proteins in hematopoietic malignancies.* Exp Cell Res, 2012. **318**(15): p. 1946-58.

144. Sekihara, K., et al., *Pifithrin-mu, an inhibitor of heat-shock protein 70, can increase the antitumor effects of hyperthermia against human prostate cancer cells.* PLoS One, 2013. **8**(11): p. e78772.

145. Ma, L., et al., *Dual targeting of heat shock proteins 90 and 70 promotes cell death and enhances the anticancer effect of chemotherapeutic agents in bladder cancer.* Oncol Rep, 2014. **31**(6): p. 2482-92.

146. Monma, H., et al., *The HSP70 and autophagy inhibitor pifithrin-mu enhances the antitumor effects of TRAIL on human pancreatic cancer.* Mol Cancer Ther, 2013. **12**(4): p. 341-51.

147. Kaiser, M., et al., *Antileukemic activity of the HSP70 inhibitor pifithrin-mu in acute leukemia.* Blood Cancer J, 2011. **1**(7): p. e28.

148. Granato, M., et al., *HSP70 inhibition by 2-phenylethynesulfonamide induces lysosomal cathepsin D release and immunogenic cell death in primary effusion lymphoma.* Cell Death Dis, 2013. **4**: p. e730.

149. Huang, C., et al., *2-phenylethynesulfonamide Prevents Induction of Pro-inflammatory Factors and Attenuates LPS-induced Liver Injury by Targeting NHE1-Hsp70 Complex in Mice.* PLoS One, 2013. **8**(6): p. e67582.

150. Ureshino, R.P., et al., *Inhibition of cytoplasmic p53 differentially modulates Ca signaling and cellular viability in young and aged striata.* Exp Gerontol, 2014. **58C**: p. 120-127.

151. Mautes, A.E., et al., *Sustained induction of heme oxygenase-1 in the traumatized spinal cord.* Exp Neurol, 2000. **166**(2): p. 254-65.

152. Reddy, S.J., F. La Marca, and P. Park, *The role of heat shock proteins in spinal cord injury.* Neurosurg Focus, 2008. **25**(5): p. E4.

153. Pan, F., et al., *[Effect of tacrolimus on apoptosis and expression of heat shock protein 70 after acute spinal cord injury in rats]*. Zhonghua Wai Ke Za Zhi, 2006. **44**(24): p. 1708-12.

154. Arranz, A., et al., *Akt1 and Akt2 protein kinases differentially contribute to macrophage polarization.* Proc Natl Acad Sci U S A, 2012. **109**(24): p. 9517-22.

155. Wang, Y.C., et al., *Notch signaling determines the M1 versus M2 polarization of macrophages in antitumor immune responses.* Cancer Res, 2010. **70**(12): p. 4840-9.

156. Wilson, H.M., *SOCS Proteins in Macrophage Polarization and Function.* Front Immunol, 2014. **5**: p. 357.

157. Saponaro, C., et al., *The PI3K/Akt pathway is required for LPS activation of microglial cells.* Immunopharmacol Immunotoxicol, 2012. **34**(5): p. 858-65.

158. Nicholas, R., et al., *Oligodendroglial-derived stress signals recruit microglia in vitro.* Neuroreport, 2003. **14**(7): p. 1001-5.

159. Nicholas, R.S., M.G. Wing, and A. Compston, *Nonactivated microglia promote oligodendrocyte precursor survival and maturation through the transcription factor NF-kappa B.* Eur J Neurosci, 2001. **13**(5): p. 959-67.

160. Wu, J., et al., *Interaction of NG2(+) glial progenitors and microglia/macrophages from the injured spinal cord.* Glia, 2010. **58**(4): p. 410-22.

161. Miller, B.A., et al., *Developmental stage of oligodendrocytes determines their response to activated microglia in vitro.* J Neuroinflammation, 2007. **4**: p. 28.

162. Hill, R.A., et al., *Modulation of oligodendrocyte generation during a critical temporal window after NG2 cell division.* Nat Neurosci, 2014. **17**(11): p. 1518-1527.

163. Ji, K., et al., *Microglia actively regulate the number of functional synapses.* PLoS One, 2013. **8**(2): p. e56293.

164. Harrison, F.E., et al., *Spatial and nonspatial escape strategies in the Barnes maze.* Learn Mem, 2006. **13**(6): p. 809-19.

165. Hitti, F.L. and S.A. Siegelbaum, *The hippocampal CA2 region is essential for social memory.* Nature, 2014. **508**(7494): p. 88-92.

166. Stevenson, E.L. and H.K. Caldwell, *Lesions to the CA2 region of the hippocampus impair social memory in mice.* Eur J Neurosci, 2014. **40**(9): p. 3294-301.

167. Uekita, T. and K. Okanoya, *Hippocampus lesions induced deficits in social and spatial recognition in Octodon degus.* Behav Brain Res, 2011. **219**(2): p. 302-9.

168. Varvel, N.H., et al., *Microglial repopulation model reveals a robust homeostatic process for replacing CNS myeloid cells.* Proc Natl Acad Sci U S A, 2012. **109**(44): p. 18150-5.

169. Michaelson, M.D., et al., *CSF-1 deficiency in mice results in abnormal brain development.* Development, 1996. **122**(9): p. 2661-72.

170. Nandi, S., et al., *The CSF-1 receptor ligands IL-34 and CSF-1 exhibit distinct developmental brain expression patterns and regulate neural progenitor cell maintenance and maturation.* Dev Biol, 2012. **367**(2): p. 100-13.

171. Erblich, B., et al., *Absence of colony stimulation factor-1 receptor results in loss of microglia, disrupted brain development and olfactory deficits.* PLoS One, 2011. **6**(10): p. e26317.

172. Byrne, P.V., L.J. Guilbert, and E.R. Stanley, *Distribution of cells bearing receptors for a colony-stimulating factor (CSF-1) in murine tissues.* J Cell Biol, 1981. **91**(3 Pt 1): p. 848-53.

173. Kodama, H., et al., *Essential role of macrophage colony-stimulating factor in the osteoclast differentiation supported by stromal cells.* J Exp Med, 1991. **173**(5): p. 1291-4.

174. Ginhoux, F., et al., *Langerhans cells arise from monocytes in vivo.* Nat Immunol, 2006. **7**(3): p. 265-73.

175. Arceci, R.J., et al., *Temporal expression and location of colony-stimulating factor 1 (CSF-1) and its receptor in the female reproductive tract are consistent with CSF-1-regulated placental development.* Proc Natl Acad Sci U S A, 1989. **86**(22): p. 8818-22.

176. Huynh, D., et al., *Colony stimulating factor-1 dependence of paneth cell development in the mouse small intestine.* Gastroenterology, 2009. **137**(1): p. 136-44, 144 e1-3.

177. Cohen, P.E., et al., *Absence of colony-stimulating factor-1 in osteopetrotic (csfmop/csfmop) mice results in male fertility defects.* Biol Reprod, 1996. **55**(2): p. 310-7.

178. Yoshida, H., et al., *The murine mutation osteopetrosis is in the coding region of the macrophage colony stimulating factor gene.* Nature, 1990. **345**(6274): p. 442-4.

179. De, I., et al., *CSF1 overexpression has pleiotropic effects on microglia in vivo.* Glia, 2014.

180. Kodama, H., et al., *Congenital osteoclast deficiency in osteopetrotic (op/op) mice is cured by injections of macrophage colony-stimulating factor.* J Exp Med, 1991. **173**(1): p. 269-72.

181. Frith, J.C., et al., *Clodronate and liposome-encapsulated clodronate are metabolized to a toxic ATP analog, adenosine 5'-(beta, gamma-dichloromethylene) triphosphate, by mammalian cells in vitro.* Journal of Bone and Mineral Research, 1997. **12**(9): p. 1358-67.

182. Sluijter, M., et al., *Inhibition of CSF-1R supports T-cell mediated melanoma therapy.* PLoS One, 2014. **9**(8): p. e104230.

183. Zhu, Y., et al., *CSF1/CSF1R blockade reprograms tumor-infiltrating macrophages and improves response to T-cell checkpoint immunotherapy in pancreatic cancer models.* Cancer Res, 2014. **74**(18): p. 5057-69.

184. Nicolaides, T.P., et al., *Targeted therapy for BRAFV600E malignant astrocytoma.* Clin Cancer Res, 2011. **17**(24): p. 7595-604.

185. Ziv, Y., et al., *Immune cells contribute to the maintenance of neurogenesis and spatial learning abilities in adulthood.* Nat Neurosci, 2006. **9**(2): p. 268-75.

186. Kipnis, J., et al., *T cell deficiency leads to cognitive dysfunction: implications for therapeutic vaccination for schizophrenia and other psychiatric conditions.* Proc Natl Acad Sci U S A, 2004. **101**(21): p. 8180-5.

187. Ron-Harel, N., et al., *Age-dependent spatial memory loss can be partially restored by immune activation.* Rejuvenation Res, 2008. **11**(5): p. 903-13.

188. Prinz, M. and J. Priller, *Microglia and brain macrophages in the molecular age: from origin to neuropsychiatric disease.* Nat Rev Neurosci, 2014. **15**(5): p. 300-12.

189. Zhan, Y., et al., *Deficient neuron-microglia signaling results in impaired functional brain connectivity and social behavior.* Nat Neurosci, 2014. **17**(3): p. 400-6.

190. Szczepanski, S.M. and R.T. Knight, *Insights into Human Behavior from Lesions to the Prefrontal Cortex.* Neuron, 2014. **83**(5): p. 1002-1018.

191. Felix-Ortiz, A.C. and K.M. Tye, *Amygdala inputs to the ventral hippocampus bidirectionally modulate social behavior*. J Neurosci, 2014. **34**(2): p. 586-95.

192. Ajami, B., et al., *Local self-renewal can sustain CNS microglia maintenance and function throughout adult life.* Nat Neurosci, 2007. **10**(12): p. 1538-43.

193. Hashimoto, D., et al., *Tissue-resident macrophages self-maintain locally throughout adult life with minimal contribution from circulating monocytes.* Immunity, 2013. **38**(4): p. 792-804.

194. Rogers, J.T., et al., *CX3CR1 deficiency leads to impairment of hippocampal cognitive function and synaptic plasticity.* J Neurosci, 2011. **31**(45): p. 16241-50.

195. Parkhurst, C.N., et al., *Microglia promote learning-dependent synapse formation through brain-derived neurotrophic factor.* Cell, 2013. **155**(7): p. 1596-609.

196. Hoshiko, M., et al., *Deficiency of the microglial receptor CX3CR1 impairs postnatal functional development of thalamocortical synapses in the barrel cortex.* J Neurosci, 2012. **32**(43): p. 15106-11.

197. Naert, G. and S. Rivest, *CC chemokine receptor 2 deficiency aggravates cognitive impairments and amyloid pathology in a transgenic mouse model of Alzheimer's disease.* J Neurosci, 2011. **31**(16): p. 6208-20.

198. El Khoury, J., et al., *Ccr2 deficiency impairs microglial accumulation and accelerates progression of Alzheimer-like disease.* Nat Med, 2007. **13**(4): p. 432-8.

199. Liu, B., et al., *Maternal hematopoietic TNF, via milk chemokines, programs hippocampal development and memory.* Nat Neurosci, 2014. **17**(1): p. 97-105.

200. Banasr, M. and R.S. Duman, *Keeping 'trk' of antidepressant actions.* Neuron, 2008. **59**(3): p. 349-51.

201. Rajkowska, G. and J.J. Miguel-Hidalgo, *Gliogenesis and glial pathology in depression.* CNS Neurol Disord Drug Targets, 2007. **6**(3): p. 219-33.

202. Raison, C.L., L. Capuron, and A.H. Miller, *Cytokines sing the blues: inflammation and the pathogenesis of depression.* Trends Immunol, 2006. **27**(1): p. 24-31.

203. Yirmiya, R., et al., *Effects of antidepressant drugs on the behavioral and physiological responses to lipopolysaccharide (LPS) in rodents.* Neuropsychopharmacology, 2001. **24**(5): p. 531-44.

204. Kreisel, T., et al., *Dynamic microglial alterations underlie stress-induced depressive-like behavior and suppressed neurogenesis.* Mol Psychiatry, 2014. **19**(6): p. 699-709.

205. Bambah-Mukku, D., et al., *A Positive Autoregulatory BDNF Feedback Loop via C/EBPbeta Mediates Hippocampal Memory Consolidation.* J Neurosci, 2014. **34**(37): p. 12547-59.

206. Hong, W., D.W. Kim, and D.J. Anderson, *Antagonistic control of social versus repetitive self-grooming behaviors by separable amygdala neuronal subsets.* Cell, 2014. **158**(6): p. 1348-61.

207. Pinkham, A.E., et al., *Neural bases for impaired social cognition in schizophrenia and autism spectrum disorders.* Schizophr Res, 2008. **99**(1-3): p. 164-75.